



AMERICAN UNIVERSITY OF BEIRUT

STUDY OF SOLAR REGENERATED MEMBRANE  
DESICCANT SYSTEM TO CONTROL HUMIDITY AND  
DECREASE ENERGY CONSUMPTION IN OFFICE SPACES

by  
KHOUDOR FAYEZ KENIAR

A thesis  
submitted in partial fulfillment of the requirements  
for the degree of Master of Mechanical Engineering  
to the Department of Mechanical Engineering  
of the Faculty of Engineering and Architecture  
at the American University of Beirut

Beirut, Lebanon  
July 2014

AMERICAN UNIVERSITY OF BEIRUT

STUDY OF SOLAR REGENERATED MEMBRANE  
DESICCANT SYSTEM TO CONTROL HUMIDITY AND  
DECREASE ENERGY CONSUMPTION IN OFFICE SPACES

by  
KHOUDOR FAYEZ KENIAR

Approved by:

Prof. Kamel Abou Ghali, PhD, Professor  
Department of Mechanical Engineering



Advisor

Prof. Nesreen Ghaddar PhD, Professor  
Department of Mechanical Engineering



Co-Advisor

Prof. Issam Lakkis, PhD, Professor  
Department of Mechanical Engineering



Member of Committee

Date of thesis defense: July 21, 2014

# AMERICAN UNIVERSITY OF BEIRUT

## THESIS, DISSERTATION, PROJECT RELEASE FORM

Student Name: Keniar Khoudor Fayez  
Last First Middle

Master's Thesis       Master's Project       Doctoral Dissertation

I authorize the American University of Beirut to: (a) reproduce hard or electronic copies of my thesis, dissertation, or project; (b) include such copies in the archives and digital repositories of the University; and (c) make freely available such copies to third parties for research or educational purposes.

I authorize the American University of Beirut, **three years after the date of submitting my thesis, dissertation, or project**, to: (a) reproduce hard or electronic copies of it; (b) include such copies in the archives and digital repositories of the University; and (c) make freely available such copies to third parties for research or educational purposes.



Signature

21-July-2014

Date

## ACKNOWLEDGMENTS

I would like to express my deepest gratitude for Dr. Kamel Abou Ghali for his advisory, guidance and patience through my graduate study.

I would also like to thank Dr. Nesreene Ghaddar for her recommendations, thoughtful ideas and help in completing this work.

Special thanks to Dr. Issam Lakkis for being a member of my thesis committee.

I would also like to thank Rami Bitar, Karim Moukalled, Roy Fattouh and Bashir El Fil for their help in performing the experiment.

I would also like to show deep gratitude to my family members and friends for their support throughout the past years.

# AN ABSTRACT OF THE THESIS OF

Khoudor Fayez Keniar for

Master of Engineering

Major: Mechanical Engineering

Title: Study of Solar Regenerated Membrane Desiccant System to Control Humidity and Decrease Energy Consumption in Office Spaces

This study investigates the feasibility of using a solar regenerated liquid desiccant membrane system to remove humidity from an internal office space. While conventional vapor compression cycles dehumidify the air before supplying it to the indoor space, through using sub cool-reheat process, the proposed cycle absorbs the humidity directly from indoor space through the dehumidifier. The dehumidifier consists of a set of permeable vertical tubes placed in the indoor space with liquid desiccant flowing through them. Solar energy is used as the source of thermal energy required for the regeneration of the desiccant and sea water is used as heat sink to provide the cooling needs of the liquid desiccant.

A mathematical model of the membrane desiccant system was integrated with the internal space model and solar systems model to predict the humidity removal capacity from the space at given dehumidification and heat sink temperatures and outdoor environmental conditions. Experiments were performed to validate the model results by comparing exit humidity and temperature of the exit air from the space.

The validated model was applied to a case study consisting of an internal office during the month of August in Beirut hot humid climate. A decrease of 10% in indoor relative humidity is observed when the system was used. The cost of the proposed system was compared to the cost of a conventional vapor compression cycle that provides the same indoor conditions. A payback period of 7 years and 8 months was estimated as compared to the investment in the vapor compression cycle.

# CONTENTS

ACKNOWLEDGMENTS.....	v
ABSTRACT.....	vi
LIST OF ILLUSTRATIONS.....	vii
LIST OF TABLES.....	viii
NOMENCLATURE.....	ix
Chapter	
I. MEMBRANE-DESICCANT SYSTEM FOR INDOOR DEHUMIDIFICATION.....	1
A. Introduction.....	1
B. Objectives.....	6
C. System Description.....	6
D. Methodology.....	8
II. INTEGRATION OF THE MEMBRANE DESICCANT SYSTEM WITH THE INDOOR AIR MODEL AND PARABOLIC COLLECTORS MODEL.....	9
A. Regenerator and Dehumidifier Mathematical Formulation.....	9
B. Indoor air Model.....	13
C. Parabolic Solar collectors Model.....	14
D. Heat Exchangers Model.....	15
E. Numerical Method and System Integration.....	16
1. Numerical Method	16
2. System Integration	17

III. EXPERIMENTAL SETUP.....	20
A. Theoretical Model.....	20
B. Experimental Description.....	21
1. Pipe Material.....	21
2. Desiccant Material.....	23
3. Experimental Setup.....	23
C. Results and Validation .....	26
IV. CASE STUDY.....	31
A. System Description... ..	31
1. Results and Performance.....	33
2. Discussion.....	35
B. Economic Analysis.....	37
1. Energy Consumption of Vapor Compression System vs. membrane System.....	37
2. Economic Analysis of Energy Consumption.....	41
C. Conclusion and Future Work.....	42
BIBLIOGRAPHY.....	45
Appendix	
I. TIME PLAN.....	50
II. CaCl <sub>2</sub> -H <sub>2</sub> O SOLUTION THERMODYNAMIC PROPERTIES.....	51
III. CONVECTION COEFFICIENTS.....	56
IV. CONSTANT RESISTANCE MODEL.....	59
V. EXPERIMENT PICTURES.....	60



## NOMENCLATURE

$T$	temperature ( $k$ )
$T_{room}$	indoor room temperature ( $k$ )
$T_{ambient}$	ambient temperature ( $k$ )
$c$	concentration of water per desiccant ( $kg_{H_2O} / kg_{CaCl_2}$ )
$c_p$	specific heat ( $J/kg \cdot k$ )
$h_c$	heat convection coefficient ( $W/m^2 \cdot s$ )
$h_m$	mass convection coefficient ( $m/s$ )
$r_o$	external radius of the pipe ( $m$ )
$r_i$	internal radius of the pipe ( $m$ )
$D$	diffusion constant of vapor in the pipe wall material ( $m^2/s$ )
$k$	thermal conductivity ( $W/m \cdot K$ )
$m$	mass rate ( $kg/s$ )
$p$	partial pressure
$n$	number of dehumidification/regeneration pipes
$l$	length of the pipe ( $m$ )
$h_{fg}$	latent heat of vaporization of the water ( $J/kg$ )
$U$	resistance coefficient of permeable pipe per unit length
$U_{total}$	resistance coefficient between the solar collectors and the ambient conditions per unit area $W/m^2 \cdot k$
$A_{total}$	area of the receiver tube in parabolic collectors ( $m^2$ )
$U_{tank}$	resistance coefficient between the storage tank and the ambient conditions per unit area $W/m^2 \cdot k$
$A_{total}$	Area of the receiver tube in parabolic collectors ( $m^2$ )
$Q$	internal heat generation ( $W$ )
$Q_{solar}$	Solar energy collected by the solar panels ( $W$ )
$Q_{load}$	Heat load of the desiccant cycle ( $W$ )
$S$	Solar flux ( $W/m^2$ )

### Greek Letters

$\rho$  density ( $\text{kg}/\text{m}^3$ )

$\omega$  humidity ratio ( $\text{kg}_{H_2O} / \text{kg}_{dryair}$ )

$\omega^*$  the equilibrium humidity ratio at surface of solution at temperature and concentration of solution ( $\text{kg}_{H_2O} / \text{kg}_{dryair}$ )

$\omega_{room}$  indoor room humidity ratio ( $\text{kg}_{H_2O} / \text{kg}_{dryair}$ )

### Subscripts

Sol  $CaCl_2$  and  $H_2O$  solution

$o$  outlet conditions

$i$  inlet supply conditions

$m$  mass convection

$c$  heat convection

$a$  air

$v$  water vapor

$w$  liquid water

## ILLUSTRATIONS

Figure 1: Schematic of the System .....	7
Figure 2: Thermal resistance model.....	12
Figure 3: Mass transfer resistance model .....	12
Figure 4: Simulation flow chart.....	18
Figure 5: Photo of the experimental setup .....	23
Figure 6: Schematic of the experimental setup.....	24
Figure 7: Pipe Assembly.....	26
Figure 8: The inlet and exit conditions to the regenerator; (a) Humidity ratio and (b) Temperature .....	27
Figure 9: The inlet and exit conditions to the dehumidifier; (a) Humidity ratio and (b) Temperature .....	28
Figure 10: Indoor temperature variation; case (A) without the membrane system, case (B) with the membrane system .....	33
Figure 11: Indoor humidity ratio variation; case (A) without the membrane system, case (B) with the membrane system .....	34
Figure 12: Indoor relative humidity variation; case (A) without the membrane system, case (B) with the membrane system .....	34
Figure 13: Thermal energy consumption of the membrane desiccant system with respect to time .....	35
Figure 14: Monthly thermal consumption of the membrane desiccant cycle.....	39
Figure 15: Storage tank temperature and solar flux hourly variation .....	40
Figure 16: Photo showing the sensors placed across the dehumidifier .....	60
Figure 17: Heating tanks.....	61

Figure 18: Permeable pipes assembly in the regenerator/dehumidifier.....	62
Figure 19: Permeable pipes assembled in the dehumidifier .....	63

## TABLES

Table 1: Comparison between experimental and theoretical.....	29
Table 2: Internal loads and Ambient Conditions .....	32
Table 3: Energy loads for the Membrane Desiccant System and Conventional System	38
Table 4: Solar system specifications.....	40

# CHAPTER I

## MEMBRANE-DESICCANT SYSTEM FOR INDOOR DEHUMIDIFICATION

### **A. Introduction**

The control of indoor humidity is of fundamental importance for building material sustainability, energy consumption and thermal comfort of indoor space occupants. Thermal comfort of the occupants involves regulating the thermal environment around them, which includes controlling temperature, air velocity and in particular humidity (Bradshaw, 2006), which will lead to maintaining a proper indoor air quality (IAQ).

Extensive research has shown that humans can withstand various levels of indoor relative humidity, where the range that is usually categorized as comfortable is between 40% to 65% in residential buildings (Wilson, 2003; Straube, 2002). Extreme level of relative humidity, whether it is high or low, can irritate people's comfort. High levels of indoor RH, exceeding 70%, hinder skin perspiration and give the person a drenched sensation, i.e. a feeling that the skin is “wetted and sticky” (Dougherty, 2011). In addition, elevated levels of relative humidity can severely deteriorate IAQ and affect the human comfort as it is the main cause of mold formation, dust mites, and different microbiological amplifications. Molds become visible on the surface of the wall, when the relative humidity exceeds 70% (Morse, et al., 2007). Similarly low levels of humidity can have negative impacts on human comfort. The human body is in discomfort when the level of relative humidity is lower than 30%) as low levels of humidity can cause several health issues, including respiratory allergic reactions, eye

irritations, skin dehydration, and dry throat and nasal passages (Bradshaw, 2006). Not only does it affect people, inappropriate levels of humidity also affect the building structure, where controlling the relative humidity has a direct effect on prolonging the endurance of the building's structure (enforcement bars, steel bars) and extending the life time service of the building itself (Ghali, et al., 2011). Negative impact of elevated moisture levels on building material includes electrochemical corrosion, volume changes, and chemical deterioration (Straube, 2002).

In order to eliminate the preceding negative impacts of elevated moisture levels, indoor humidity should be controlled. Humidity control is usually accomplished by two methods: conventional and non-conventional techniques. In environments with high temperature and humidity, the conventional way of moisture removal is cooling the supply air to a temperature below its dew point to condense the excess moisture followed by reheating to the adequate supply air temperature. Alternatively, one can use desiccant dehumidification as a less energy consuming process. Both processes require energy to control the level of humidity and thus the two processes are classified as energy active methods for moisture removal.

The continuous increase in energy demand and costs, added to the associated environmental problems resulting from energy generation (ex. Global warming), turned the attention of researchers towards considering non-conventional and passive methods for controlling indoor humidity. A very intriguing technique uses the attic, lined with plywood, as a dehumidifier chamber. During the night, the attic wood material will dehumidify the space air and during the day the solar energy will remove the attic-absorbed moisture. Although this system is not an active energy consuming system, it is inefficient in terms of time and space. The regeneration of the air is done during the day

while what is needed during the day is the dehumidification process. It also requires a huge space, which is the attic, to operate (Chenvidyakarn, 2007). A similar passive technique that allows an occupied room to get dehumidified is by the use of a “double-glazing window unit, whose gap is filled with louvres coated with a silica powder desiccant”. This technique is similar to dehumidification using the attic of the house. It dehumidifies during the night and regenerates during the day (Chenvidyakarn, 2007).

The preceding dehumidification techniques, conventional compression cycle, desiccants and attic plywood, have many negative side effects. The drawback of using the glazing window or the attic as a dehumidification chamber is that dehumidification is occurring during the night while what is required is day time dehumidification when the indoor latent load is high. As for conventional vapor compression and desiccant cycles, both are bulky systems; requiring heating coil and oversized cooling system for vapor compression and dehumidification and regeneration tower beds when using liquid desiccant systems and two rotating wheels (dehumidification and sensible) when using solid desiccant (La, et al., 2010). All of these components require adequate space that might not be available in residential apartments. As for energy considerations, the vapor compression cycle consumes electric energy as the main source of energy which causes many economic and environmental negative impacts. On the other side, although liquid desiccant technology is considered an active method, it can be integrated with sustainable energy sources to reduce the electricity consumption associated with regulating indoor humidity and temperature. Nonetheless, there are many issues that rise from using liquid tower beds; the first is the direct contact of air with the liquid desiccant which might cause health issues and corrosion problems (Studak, et al., 1988) especially with the entrainment of hazardous salts to the ventilation system. The second



issue is that in dehumidifying the supply air outside the indoor space, the humidity ratio must be further lowered to below indoor space humidity ratio; this requires a strong desiccant solution. The third issue is that dehumidifying the supply air outside the indoor space will not respond directly to internal latent load changes and is an efficient technique as shown by recent developments (Fauchoux, et al., 2010) (Eldeeb, et al., 2013).

To overcome the preceding negative effects of the dehumidification methods, a novel technique has been recently developed that is the Heat and Moisture Transfer Panel (HAMP) (Fauchoux, et al., 2009) (Fauchoux, et al., 2010) (Eldeeb, et al., 2013). The HAMP is able to control temperature and indoor relative humidity (Fauchoux, et al., 2010) using liquid desiccant as the working fluid. The desiccant circulates in a cycle, where it absorbs humidity from the indoor room through a permeable membrane eliminating the need for the dehumidification tower bed. Following the dehumidification process and to complete the desiccant cycle, the desiccant should be regenerated. The HAMP study (Fauchoux, et al., 2010) focused on the dehumidification process and did not consider the ability of the membrane material to regenerate the desiccant. The use of the membrane material to both air dehumidification and liquid desiccant regeneration will not only eliminate the conventional liquid desiccant dehumidification tower but also the regeneration tower leading to a less bulky humidity control system, in contrary to conventional liquid desiccant humidity control cycles (Mohammad, et al., 2013). Another technique that uses the permeable membrane technology is the RAMEE (Run Around Membrane Energy Exchanger) (Mahmud, et al., 2010) (Moghaddam, et al., 2013). The RAMEE was tested in a closed loop system and proved to be efficient (Hemingson, et al., 2011), but it substitutes the

dehumidification and regeneration tower beds as it performs outdoor air dehumidification.

The cooling needs of the desiccant cycle in passive dehumidification methods is still a major issue that this technology needs to overcome (Mohammad, et al., 2013). However, in some countries where there is an available heat sink and there is a need for indoor air dehumidification, desiccant systems become an attractive substitute for conventional HVAC systems. In particular, permeable membrane dehumidification might have an advantage over conventional vapor compression cycles, as the thermal energy required for it can be met through using solar energy and the cooling is done through using the available heat sink. This will lead to reduction in electric energy consumption and thus will have positive economic and environmental outcomes.

This study investigates the use of a solar-regenerated membrane desiccant system to dehumidify a typical internal office space in the city of Beirut. Beirut suffers from high humidity levels during the summer time, thus efficient dehumidification techniques are needed during that period. The fact that Beirut is a coastal city where sea water can be used as a heat sink (Audah, et al., 2011) in addition to the availability of solar radiation throughout the summer makes it an attractive candidate for the application of the passive membrane dehumidification system. To achieve the objectives stated, the desiccant membrane system will be integrated with the internal space model and solar panels model. After evaluating the feasibility of the system to provide thermal comfort, it will be compared to conventional HVAC systems in the existence of a heat sink. The energy consumption of both systems will be evaluated in order to determine which dehumidification process requires less energy and hence lower cost of initial installation or cost of electricity.

## **B. Objectives**

The following are the objectives to be achieved from this study:

1. Derive a mathematical model for a solar energy-based system that dehumidifies indoor zones
2. Validate the mathematical regeneration model by conducting experiments
3. Integrate the proposed dehumidification system with the indoor air modal and parabolic collectors and apply it to a case study for the city of Beirut
4. Compare the energy consumption and cost of the membrane system with the conventional vapor compression air conditioning system

## **C. System Description**

The proposed dehumidification system is composed of the dehumidification permeable pipes, desiccant regeneration permeable pipes, sensible heat exchangers, regeneration heat exchanger, and parabolic solar collectors. Fig.1 illustrates the system components. The membrane-desiccant system will control the space relative humidity, while the heat sink source will be used to cool the air before it enters to the room. The piping system is made of solid piping lines except in the regenerator and dehumidifier parts. In those sections the main pipe is divided to many pipes where each is made of a porous material, polypropylene-commercial name Propore<sup>®</sup>, which is permeable to water vapor but not liquid. The permeable pipes are put inside the indoor space to absorb the moisture from the air and hence perform direct indoor dehumidification. A similar set of pipes will be exposed to the ambient air in order to regenerate the liquid desiccant. The regeneration permeable pipes will not be subjected to direct sunlight-

especially UV rays- and they will be put in shades in case they are exposed to ambient air (Larson, 2006).

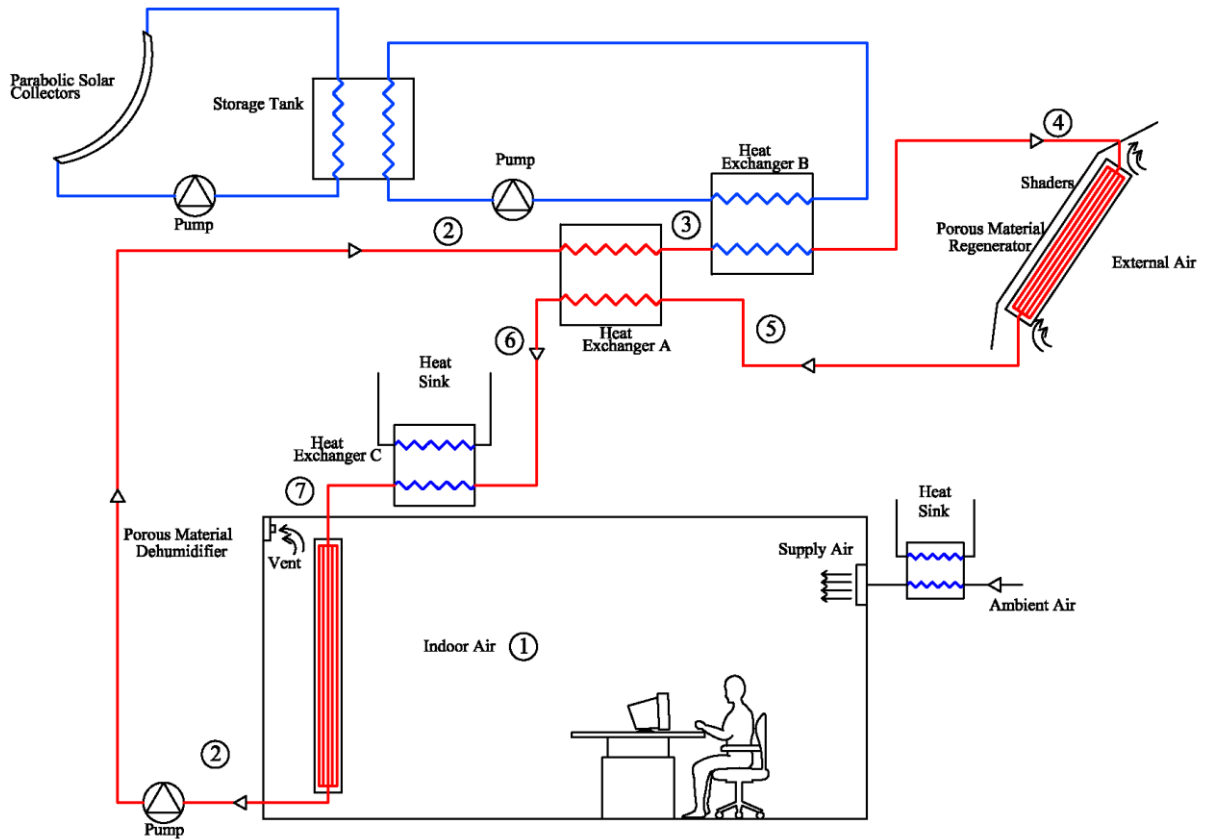


Figure 1: Schematic of the System

The close loop cycle starts as follows. The cool strong liquid desiccant enters the permeable-membrane pipes at (7) picking the moisture from the indoor space (1) to leave at (2) where it is pumped through a solid piping. The desiccant solution then gets heated from the high temperature desiccant leaving the regenerative membrane (exchanger A) and solar energy stored in the tank (exchanger B). The heated desiccant then enters the regenerator, at (4), i.e. the permeable pipes in contact with ambient air. It will then loose the absorbed indoor moisture to the external ambient environment. To ensure that the desiccant will not impose an additional sensible indoor heat source and to increase its ability in picking the indoor moisture, the desiccant will first exchange

heat with the cool desiccant solution leaving indoor room (exchanger A), then it will be further cooled through the heat sink (exchanger C). After passing through exchanger (C) the desiccant enters the dehumidifier again at (7).

The liquid desiccant needs to be heated (regenerated) in order to expel the moisture it absorbed from the indoor environment. The energy source required for regeneration will be solar energy. The solar irradiance will be collected through parabolic plate collectors which will heat a working fluid, which in turn will transfer the heat and store it in a storage tank to be supplied continuously to the membrane desiccant cycle.

#### **D. Methodology**

The membrane desiccant cycle is modeled and simulated to study its efficiency in dehumidifying indoor space. Steady state and 1-D models for the different cycle subsystems; dehumidification pipes, regeneration pipes and heat exchangers are developed. The liquid desiccant membrane cycle is integrated with the quasi-steady state space model to predict the performance of the proposed system in controlling the space relative humidity.

Following the model development, experimental tests are conducted to validate the mathematical model and its ability in predicting humidity removal from the space. Then the system will be applied to a case study where its performance in Beirut City is evaluated and compared to vapor compression cycles.

## CHAPTER II

### INTEGRATION OF THE MEMBRANE DESICCANT SYSTEM WITH THE INDOOR AIR MODEL AND PARABOLIC COLLECTORS MODEL

To study the effect of the desiccant membranes in controlling the indoor humidity, the membrane dehumidification and regeneration stages in the full cycle will be integrated with the parabolic solar collector system and the space thermal model. The full system cycle is shown in Fig 1. For a given sensible and latent space load, the integrated model will assess the performance of the hybrid air conditioning system in decoupling the space temperature and humidity control.

There are 3 main subsystems in the cycle to model. The first is the liquid desiccant/permeable membrane model in the regenerator and dehumidifier, the second is the indoor room model and the last is the parabolic solar collector model.

#### **A. Regenerator and Dehumidifier Mathematical Formulation**

The dehumidifier/regenerator consists of the liquid desiccant in the permeable pipes. It couples the heat and mass transfer between the desiccant and the surrounding air. There are two variables that must be calculated through the model which are the temperature and concentration of the desiccant solution.

Many models in the literature are used to derive the temperature and concentration variation of liquid desiccants, some of which are mentioned in (Bergero, et al., 2001) (Radhwan, et al., 1993) (Elsayed, et al., 1993) (Fumo, et al., 2002). Most of the modeling techniques of liquid desiccants are found in the context of

dehumidification/cooling towers (Radhwan, et al., 1993) (Elsayed, et al., 1993) (Fumo, et al., 2002) where there is direct contact between the air and the desiccant. The case under study is different from that of the dehumidification towers, in which there is no direct liquid-vapor interface but a permeable membrane that separates the two phases. The mass and energy equations developed for the permeable pipes will follow the model developed by (Bergero, et al., 2001) (Fan, et al., 2006) (Fauchoux, et al., 2010). The derived model is specifically similar to (Bergero, et al., 2001) where there is a liquid desiccant flowing inside a pipe-in-particular capillary tube- with permeable walls that allow vapor transfer but prohibits liquid water penetration.

In order to predict how the temperature and the concentration will vary inside the pipe, conservation laws of energy and mass are applied under restricting assumptions. The equations were derived under the assumption of 1-D heat and moisture variation, no energy or mass storage in the pipe membrane, i.e. quasi-equilibrium model, the liquid desiccant solution is assumed to be ideal, the mechanism of vapor transport in the membrane is only due to diffusion, the axial heat conduction and vapor diffusion in the pipe are neglected, The variation of latent heat with temperature is neglected

The mass flow on dry basis, i.e. the desiccant,  $CaCl_2$ , flow rate per second, is assumed constant in the pipes while the total mass flow rate is variable due to absorption or desorption of liquid water. In order to proceed with the derivation of the model, the thermo-physical properties of the pipe material should be known. These properties include the vapor permeability and the thermal conductivity of the material. The material chosen is micro porous polypropylene, Propore<sup>®</sup>, for which the properties

can be found in (Larson, 2006). The liquid desiccant,  $CaCl_2 - H_2O$  solution, properties follow the correlations given in (Conde, 2004), Appendix A.

Applying the above assumptions, the energy equation is then given by

$$0 = -m_d \frac{d}{dy} \{h_{sol}(1+c_{sol})\} + U_c (T_o - T_{sol}) + h_{fg} \rho_a U_m (\omega_0 - \omega_{sol}^*) \quad (1)$$

The first term on the right represents the net convective energy flow and the second term represents sensible energy added to the solution due to difference in temperature between liquid desiccant and the surrounding air temperature. The last term represents the energy added due to the absorption of moisture into the solution. The overall heat and mass transfer coefficients,  $U_c$  and  $U_m$ , per unit length (Appendix C), are represented by

$$U_c = \left\{ \frac{1}{2\pi r_o h_{c,o}} + \frac{\ln(r_o/r_i)}{2\pi k} + \frac{1}{2\pi r_i h_{c,i}} \right\}^{-1} \quad (2)$$

$$U_m = \left\{ \frac{1}{2\pi r_o h_{m,o}} + \frac{\ln(r_o/r_i)}{2\pi D} + \frac{1}{2\pi r_i h_{m,i}} \right\}^{-1} \quad (3)$$

Equations (2) and (3) couple the membrane properties of the pipe with the flow properties on both sides of the membrane as shown in Figures 2 and 3. The values of the convection coefficients are determined according to the correlations shown in Appendix B.

The species conservation equation for the permeable pipes is

$$0 = -m_d \frac{dc}{dy} + \rho_a U_m (\omega_0 - \omega_{sol}^*) \quad (4)$$



The first term on the right represents the net moisture convective flow and the second term represents the moisture transfer from the surrounding air to the solution in the pipe, across a concentration difference of  $(\omega_0 - \omega_{sol}^*)$ .

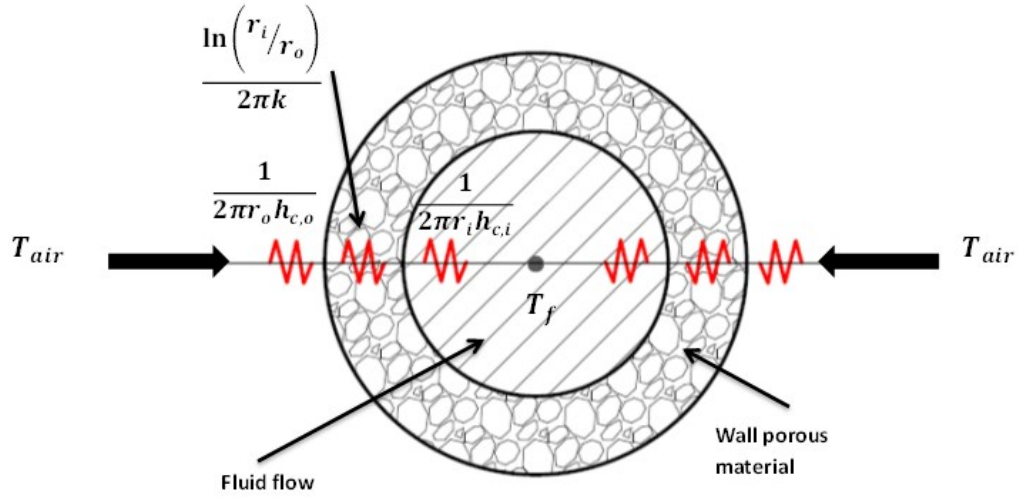


Figure 2: Thermal resistance model

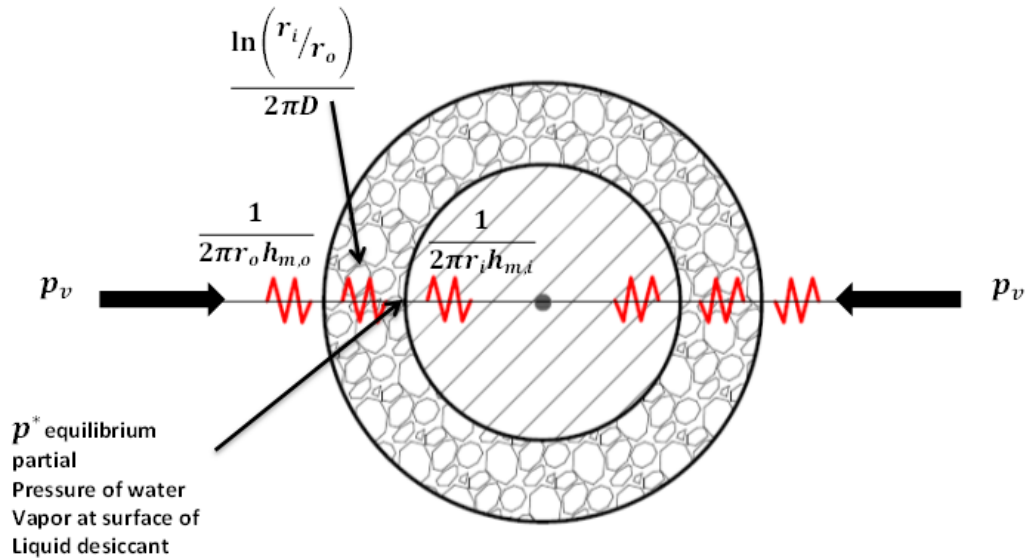


Figure 3: Mass transfer resistance model

The humidity ratio in the surrounding air is  $\omega_0$  while  $\omega_{sol}^*$  is the equilibrium humidity of the liquid desiccant at the solution's temperature and concentration,  $T_{sol}$  and

$c_{sol}$  respectively. This is usually calculated from equilibrium isotherms found for combinations of desiccants and fluids at different temperatures and concentrations (Appendix A).

## B. Indoor Air Model

The indoor space has a single input air flow that is conditioned only for sensible load with no latent load, i.e. the temperature of the air is reduced to a temperature that is below the dew point temperature with no reheat using the available heat sink. The indoor room has a single output vent.

In this study, a model for indoor space is developed following the work done in (Yassine, et al., 2012) under the following assumptions: quasi steady state where a steady state model for the room is used with time varying internal loads. The lumped air approach is used, thus solving for the average temperature and humidity of the room. Ideal gas model for the equation of state of air and water vapor is used. The loads are mostly internal with no external loads, and minimal heat transfer occurs across the room walls, and hence the room is assumed to have adiabatic walls. The space represents an internal office room in a typical firm in Beirut City.

Applying the above assumptions and knowing the flow rate and the conditions of the supplied air, the space energy equation can be written as

$$m_a c_{pa} (T_i - T_o) + m_a c_{pv} (T_i \omega_i - T_o \omega_o) + Q = \sum_{i=1}^n \int_0^{l_i} U_c (T_o - T_{sol}) dy \quad (5)$$

where the first two terms on the left side of the equation represent the convective sensible heat flows, of dry air and water vapor respectively, and the last term represents

the space internal load (sensible). The term on the right side of the equation represents the sensible energy transfer with the set of desiccant membrane pipes found in the indoor space. The summation operator is due to the fact that we might have different pipes operating in a room each with a different length. The integration is done over the whole length  $l$  of each pipe to take into consideration the variation of temperature in the pipe.

Similarly, the space moisture balance equation can be represented as

$$m_a(\omega_i - \omega_o) + m_g = \sum_{i=1}^n \int_0^{l_i} U_m \rho_a (\omega_o - \omega_{sol}^*) dy \quad (6)$$

The two terms on the left side of the equation represent the convective moisture transfer and the internal moisture generation. The right side of the equation represents the moisture exchange with the desiccant membrane piping system.

### C. Parabolic Solar Collectors Model

The energy required for regeneration of the liquid desiccant will be supplied from the solar irradiance. Parabolic solar collectors will be used to harvest the solar energy and supply the required heat for the cycle. The model for the solar collector with storage tank has been extensively researched in literature. The model developed by (Duffie, et al.) will be used in this proposal. It will be integrated with the other subsystems in the cycle to form the total numerical modal which is used in the simulations.

The heat gained in the solar collectors is found through the following equation:

$$Q_{solar} = SA_r - U_{total} A_r (T_{avr} - T_{ambient}) \quad (7)$$

where  $S$  is the solar flux, as a function of time, supplied to the receiver pipe passing through the focal point of the parabolic collectors.  $A_r$  is the area of the receiver pipe and  $U_{total}$  is the heat loss coefficient associated with average temperature of the fluid inside,  $T_{avr}$ , and ambient temperature of the surrounding air,  $T_{ambient}$ .

This heat supplied is stored in the storage tank, having the following transient equation:

$$\rho_w c_{p,w} \frac{dT}{dt} = Q_{solar} - Q_{load} - U_{tank} A_{tank} (T_{tank} - T_{ambient}) \quad (8)$$

The tank is used to store thermal energy to be used when the dehumidification cycle is running.  $\rho_w, c_{p,w}$  are the density and specific heat of water respectively.  $V$  is the tank volume and  $U_{tank}$  is the heat loss coefficient of the tank associated with the temperature of the tank inside,  $T_{tank}$ , and the ambient air temperature,  $T_{ambient}$ .  $Q_{load}$  is the thermal load of the dehumidification cycle required each hour in the cycle.

#### **D. Heat Exchangers Model**

The model for the heat exchangers will use the effectiveness-NTU method and hence known efficiency for the heat exchangers (Incropera, et al.). The heat exchangers are used in three stages in the cycle. The first heat exchanger, exchanger B in Fig. 1, is used to supply thermal energy to the liquid desiccant in order to raise its temperature to the required regeneration temperature. The second heat exchanger, exchanger A in fig.1, is used for regeneration heat exchange with the cool liquid desiccant leaving the indoor space. The last heat exchanger is used to lower the temperature of the liquid desiccant entering the room through exchanging heat with the heat sink.

The following model is used for the heat exchangers:

$$Q_{\max} = (mc_p)_{\min} (T_{hot,in} - T_{cold,in}) \quad (9)$$

$$T_{hot,out} = T_{hot,in} - \varepsilon \frac{Q_{\max}}{(mc_p)_{hot}} \quad (10)$$

$$T_{cold,out} = T_{cold,in} - \varepsilon \frac{Q_{\max}}{(mc_p)_{cold}} \quad (11)$$

In the above equations,  $mc_p$  is the minimum heat capacity of the two fluids entering the heat exchanger,  $T_{hot,in}$  is the temperature of the hot fluid entering the heat exchanger and  $T_{cold,in}$  is the temperature of the cold fluid entering the heat exchanger.  $Q_{\max}$  is the maximum possible heat transfer, and  $\varepsilon$  is the effectiveness of the heat exchanger.

## E. Numerical Method and System Integration

### 1. Numerical Method

The equations governing mass and heat transfer across the permeable membrane forming the dehumidifier/regenerator tubes are discretized according to the finite difference scheme. The mass and energy equations are solved simultaneously for the concentration and temperature of the  $i^{\text{th}}$  element.

Energy and species balance equations:

$$\left\{ \begin{array}{l} c_i + \frac{\Delta y U_m \rho_a}{m_d} (\omega_{sol}^*(c_i, T_i) - \omega_o) - c_{i-1} = 0 \\ (1 + c_i) h_{sol}(T_i, c_i) + \frac{\Delta y U_c \rho_a}{m_d} (T_i - T_o) + \frac{\Delta y U_m \rho_a h_{fg}}{m_d} (\omega_{sol}^*(c_i, T_i) - \omega_o) - (1 + c_{i-1}) h_{sol}(T_{i-1}, c_{i-1}) = 0 \end{array} \right\} \quad (12)$$

Knowing the material properties and dimensions, the temperature and humidity ratio of the surrounding air,  $T_o$  and  $\omega_o$  respectively, and the temperature and concentration at the

previous element, “i-1” element in the tube, the temperature and concentration at the  $i^{\text{th}}$  element can be calculated by solving the above system of nonlinear equation at each element “i” simultaneously using Newton Raphson Technique as a numerical method for solving the system. The correlations for  $\omega_{sol}^*$  and  $h_{sol}$  are shown in appendix A. The boundary conditions, i.e. the temperature and concentration at element “i=1” are given by the inlet temperature and concentration of the liquid desiccant entering the dehumidifier in the indoor space or regenerator.

## ***2. System Integration***

In order to simulate the performance of the membrane desiccant system in dehumidifying the indoor space, the following input conditions are needed: the dimensions and the physical and thermal properties of the permeable pipes, the internal sensible and latent load profile, the ambient conditions, the supply conditions of the air to the indoor space, the temperature, mass concentration and the mass flow rate of the desiccant solution entering the indoor space through the permeable pipes. The finite difference method will be used to solve for the temperature and concentration variation of the pipes in the room, under steady state assumptions. The dehumidification and regeneration pipes are discretized into 100 elements in order to account for the temperature and concentration variation throughout the length of the pipe. Any further increase in the number of elements of the pipes did not lead to improvement in results. The average temperature and humidity in the indoor space is calculated using the developed model. The storage tank that couples the solar system and the desiccant system is simulated using transient explicit scheme with lumped temperature model.

The solution flow chart is shown in Fig. 4. Simulations start by setting the input conditions to the cycle. Then using the dehumidifier and the internal space model the room temperature, humidity ratio and the exit temperature and concentration of the dehumidifier are calculated.

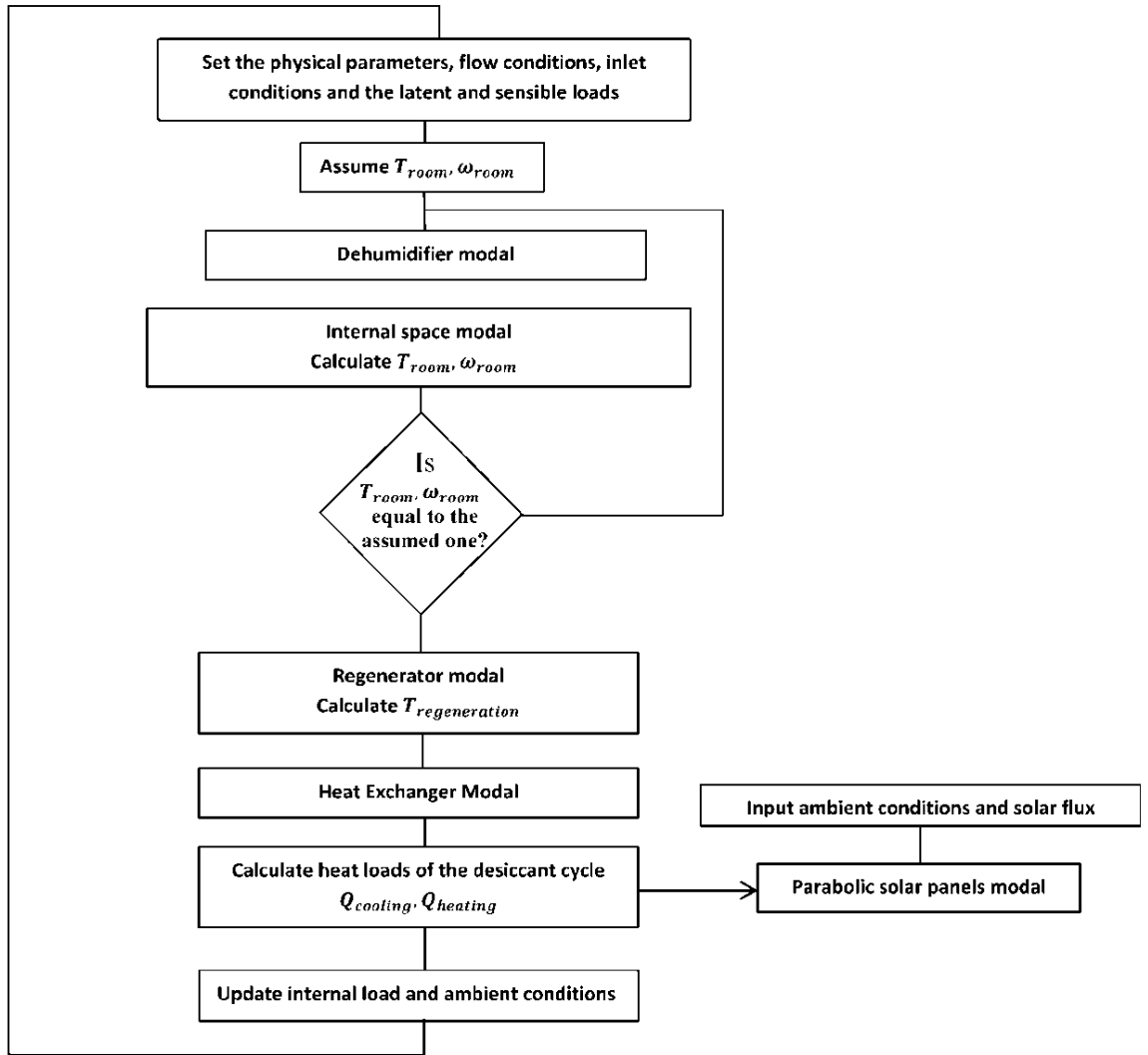


Figure 4: Simulation flow chart

To regenerate the desiccant, the regenerator model is used to calculate the required regeneration temperature of the cycle. Using the same model, the exit temperature of the regenerator is also calculated. Knowing the inlet and exit temperatures at the

regenerator and dehumidifier, the cooling and heating needs of the desiccant cycle are evaluated through the heat exchanger model. The resulting regeneration energy along with the solar flux during the day, are used as an input to the solar system in order to calculate the storage tank temperature. The simulations of the tank will run for a period of one day. The program used for solution is MATLAB<sup>®</sup>.



## CHAPTER III

### EXPERIMENTAL SETUP

To test the regeneration and absorption ability of the permeable membrane used in the study and to validate the theoretical model, an experimental setup was built. The setup was composed of a membrane dehumidifier, membrane regenerator, heat exchanger, and heating tank.

#### A. Theoretical Model

The dehumidifier/regenerator duct is consists of a concentric tube heat and mass exchange setup. The dehumidifier is formed of four permeable tubes placed inside an air duct. In order to validate the mathematical formulation, the vapor absorbed by the dehumidifier and that desorbed by the regenerator are to be predicted by the theoretical model and compared to the experimental results. The mass and heat balance equations that govern the variation of the temperature and concentration of the liquid desiccant are equations (1) and (2) respectively. As for the air side, the heat and mass balance equations are developed according to symmetric boundary conditions between the tubes and using the constant resistance modal developed earlier in equations (3) and (4). The conservation of energy becomes:

$$m_a \frac{d}{dy} \{c_{p,a} T_a + \omega(c_{p,v} T_a + h_{fg})\} = U_c (T - T_a) + U_m \rho_a h_{fg} (\omega_{sol}^*(T, c) - \omega) \quad (13)$$

The term on the left represents the change of enthalpy of air across a control volume. The first term on the right represents the sensible heat transfer between the air and the liquid desiccant in the pipes. The second term represents latent heat transfer

between the liquid desiccant and the pipes due to mass transfer. The species balance for the air side is:

$$m_a \frac{d\omega}{dy} = U_m \rho_a (\omega_{sol}^*(T, c) - \omega) \quad (14)$$

where this equation balances the change in water vapor content of the air to how much has been transferred to (or from) the liquid desiccant.

## **B. Experimental Description**

### ***1. Pipe Material***

The pipe material choice is of fundamental importance. The material should be permeable to water vapor with high permeability compared to other material and simultaneously impermeable to liquid water, i.e. it should have a high liquid penetration pressure. The material should endure high temperatures to withstand the regeneration temperature of the desiccant solution in the regeneration pipes. An additional economic requirement is that the material should be of low cost. The required system/cycle should be economically feasible compared to other dehumidification methods.

In summary the required material should have the following features: Permeable to water vapor and impermeable to liquid water, endures high temperatures, and economically cheap.

There are several materials that satisfy to some degree one or more of the required features. The materials that were included are the following:

1. Tyvek<sup>®</sup>
2. Propore<sup>™</sup> Polypropylene (PP)

3. Teflon<sup>®</sup>ePTFE

4. Sympatex<sup>®</sup> Membrane

Based mainly on the research done by Larson (Larson, 2006) in his master's thesis, the preferred material for our application is Propore<sup>®</sup> (Microporous polypropylene membrane) which has high water vapor permeability. This material has been used in previous similar applications (Larson, 2006) (Fauchoux, et al., 2010). Propore<sup>®</sup> or Microporous polypropylene (PP) membrane has high water vapor permeability while preventing liquid penetration (high liquid penetration pressure). It has a melting temperature ranging between 135°C and 159°C. Upon prolonged exposure to UV rays, the mechanical properties of Propore<sup>®</sup> deteriorate and the surface roughness increases (Larson, 2006).

#### *Permeability*

In order to determine the permeability (diffusivity) of the material to water vapor, an experiment will be carried in the lab. In the experiment, a cup filled with water will be placed on a balance. The cup top will be perfectly sealed with the Propore<sup>®</sup>, such that the only exchange of water vapor will be through the membrane. The mass of the cup will be recorded with time until the mass change is constant and hence steady state is reached. Then the temperature of the water is measured and temperature and relative humidity of the air at the top of the membrane is also measured, from these measurements the partial pressure of water vapor in the air and at the surface of the water can be determined. After measuring the mass flow rate of water vapor and the pressure difference across which this flow happens, the resistance to the flow and hence the permeability of the membrane can be determined. It was compared to data published in literature and the values conformed.

## 2. Desiccant Material

The desiccant material used in the  $CaCl_2$ . Similar humidification-dehumidification systems have used other desiccants such as Lithium Chloride and Lithium Bromide (Radhwan, et al., 1993) (Ghaddar, et al., 2004) (Pa'tek\*, et al., 2006). Calcium Chloride is chosen because it is one of the most common working fluid in absorption systems (Conde, 2004). Its moisture absorption capability and low corrosiveness along with its cheap price makes it an attractive candidate for such applications.

## 3. Experimental Setup

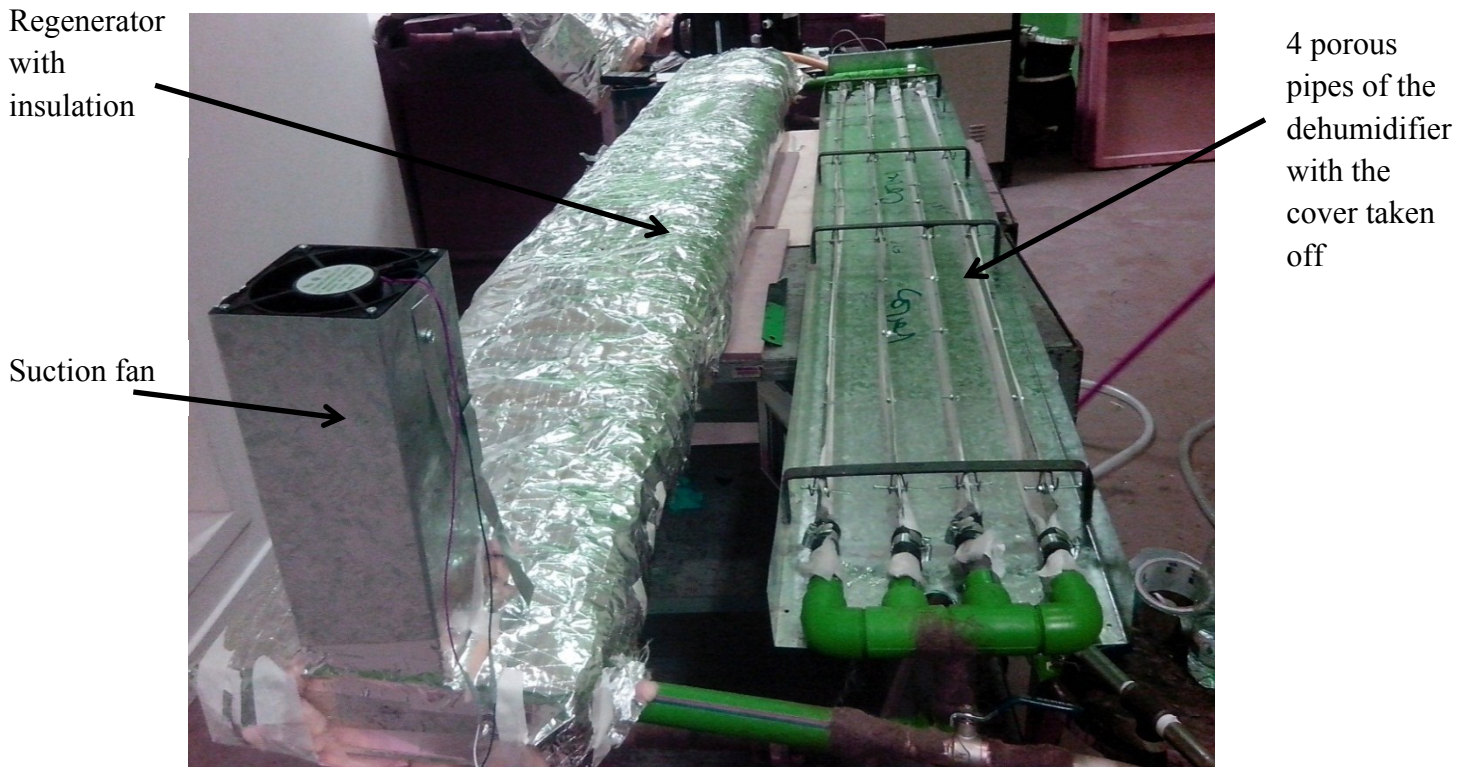


Figure 5: Photo of the experimental setup

The experimental setup build to test the absorption ability of the membrane and to validate the mathematical formulation is composed of a membrane dehumidifier,

membrane regenerator, heat exchanger, and heating tank, a photo of the system is shown in Fig. 5. The supply air to the dehumidifier and regenerator was supplied from two different environmental chambers.

A schematic of the experimental setup showing the regenerator tubes, dehumidifier tubes, heating tank and cooling heat exchanger is shown in Fig. 6.

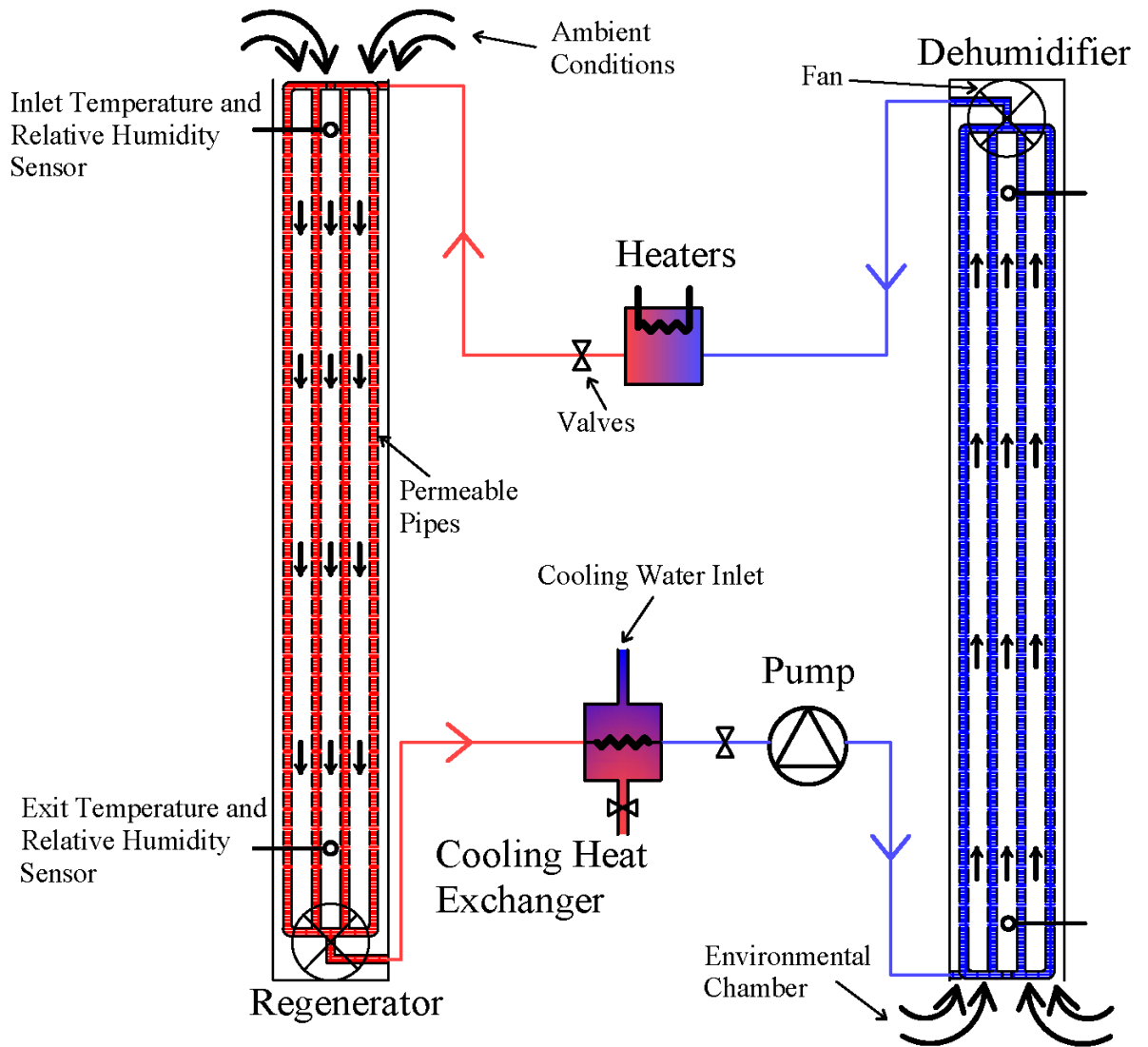


Figure 6: Schematic of the experimental setup

The dehumidifier and regenerator tubes are enclosed in a rectangular air duct of length 2 m and a cross section of 7×30 cm with controlled suction fans at the end. Inside

the air ducts there are four cylindrical pipes made from Propore<sup>®</sup> material. The pipes are manufactured through cutting a rectangular piece of Propore<sup>®</sup> of length 1.36 m and 6.3 cm in width. The rectangular piece is then folded along the width to form a cylinder of diameter  $2 \pm 0.1$  cm and length  $1.36 \pm 0.01$  m. Two metallic sheets are pressed along the top part of the rectangular piece and held together by small clamps in order to give the pipes the cylindrical shape and keep them intact once the liquid desiccant passes through them, as shown in Fig. 6. The working fluid in the setup is a liquid desiccant solution made of  $CaCl_2$  and water with a concentration of  $38 \pm 1$  %. The flow rate of the desiccant was set to 69 L/hour and measured through a stop watch and graduated cylinder. The desiccant temperature entering the regenerator was controlled through a PID controller (Delta D series temperature controller modal DTD4848V0) and was set at 39°C with a  $\pm 1^\circ\text{C}$  steady state error from the set value. The controller was applied to the heating tank which has a heating capacity of 2200 Watts and total volume of 6 liters. The temperature of the desiccant entering the dehumidifier was controlled through monitoring the flow of chilled water to the heat exchanger. The temperature at the inlet of the dehumidifier was set at 24°C and measured through a type K thermocouple (connected to an OMEGA<sup>®</sup> HH21 Microprocessor Thermometer); the error in the reading is  $\pm 0.5^\circ\text{C}$ .

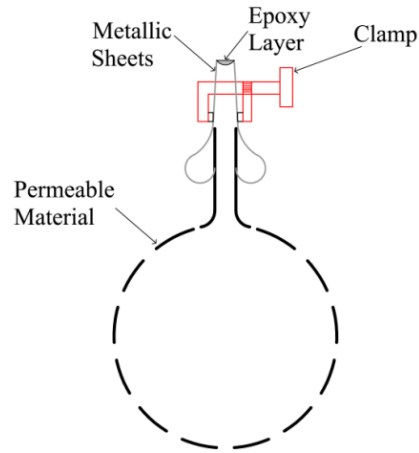


Figure 7: Pipe Assembly

The air at the inlet of the dehumidifier duct will be supplied from an environmental chamber maintained at a mean fixed temperature of  $25.8^{\circ}\text{C} \pm 0.3$  and mean humidity ratio of  $17.45 \text{ g}_w/\text{Kg}_a \pm 0.65$ . The inlet air at the regenerator will be taken from the lab environment at  $24.5^{\circ}\text{C} \pm 0.3$  and mean humidity ratio of  $12.38 \pm 0.54 \text{ g}_w/\text{Kg}_a$ . Sensors at the inlet and exit of the air flow in the dehumidifier and regenerator are added to monitor the properties of the air and hence calculate the mass and heat transfer to it. The sensors used are OMEGA<sup>®</sup> HX94A Series Humidity/Temperature sensors with relative humidity accuracy of  $\pm 2.5\%$  and temperature accuracy of  $\pm 0.3^{\circ}\text{C}$ . The sensors were connected to a data acquisition system (OM-DAQPRO-5300) which is used to process the input data of the sensors. The mass flow rate of the air in the dehumidifier/regenerator was calculated through measuring the velocity through an anemometer (BK PRECISION model 731A), with error of 3% of the reading. The air mass flow rate was set at  $1.12 \text{ g/s}$  by controlling the speed of the suction fans.

### C. Results and Validation

After turning on the fans and the pump and regulating the cooling water valves, the sensors were turned on to take the readings. The testing setup was left to operate for 4 hours. The measurements were saved after watching the temperature and humidity ratio at the exit of the dehumidifier and regenerator stabilize. The measurements taken for the inlet and exit conditions of the regenerator and dehumidifier are shown in figures 8 and 9 respectively.

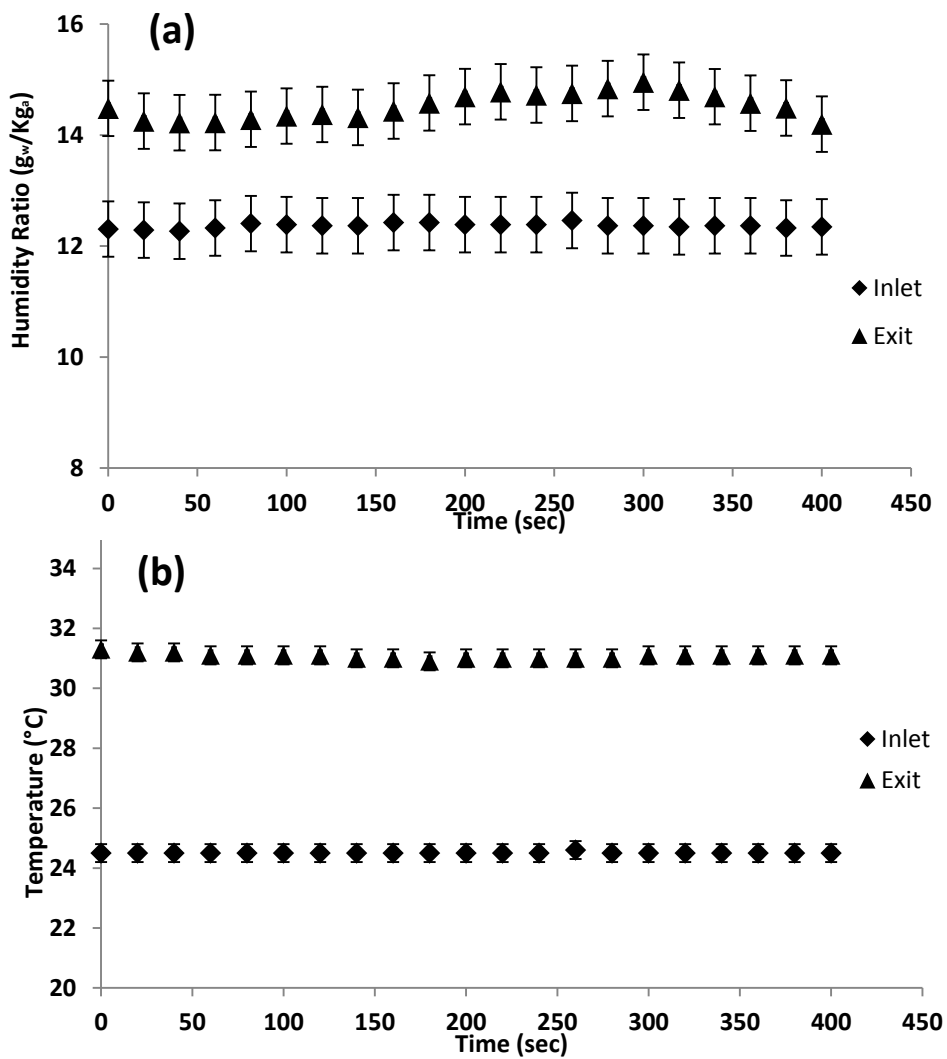


Figure 8: The inlet and exit conditions to the regenerator; (a) Humidity ratio and (b) Temperature



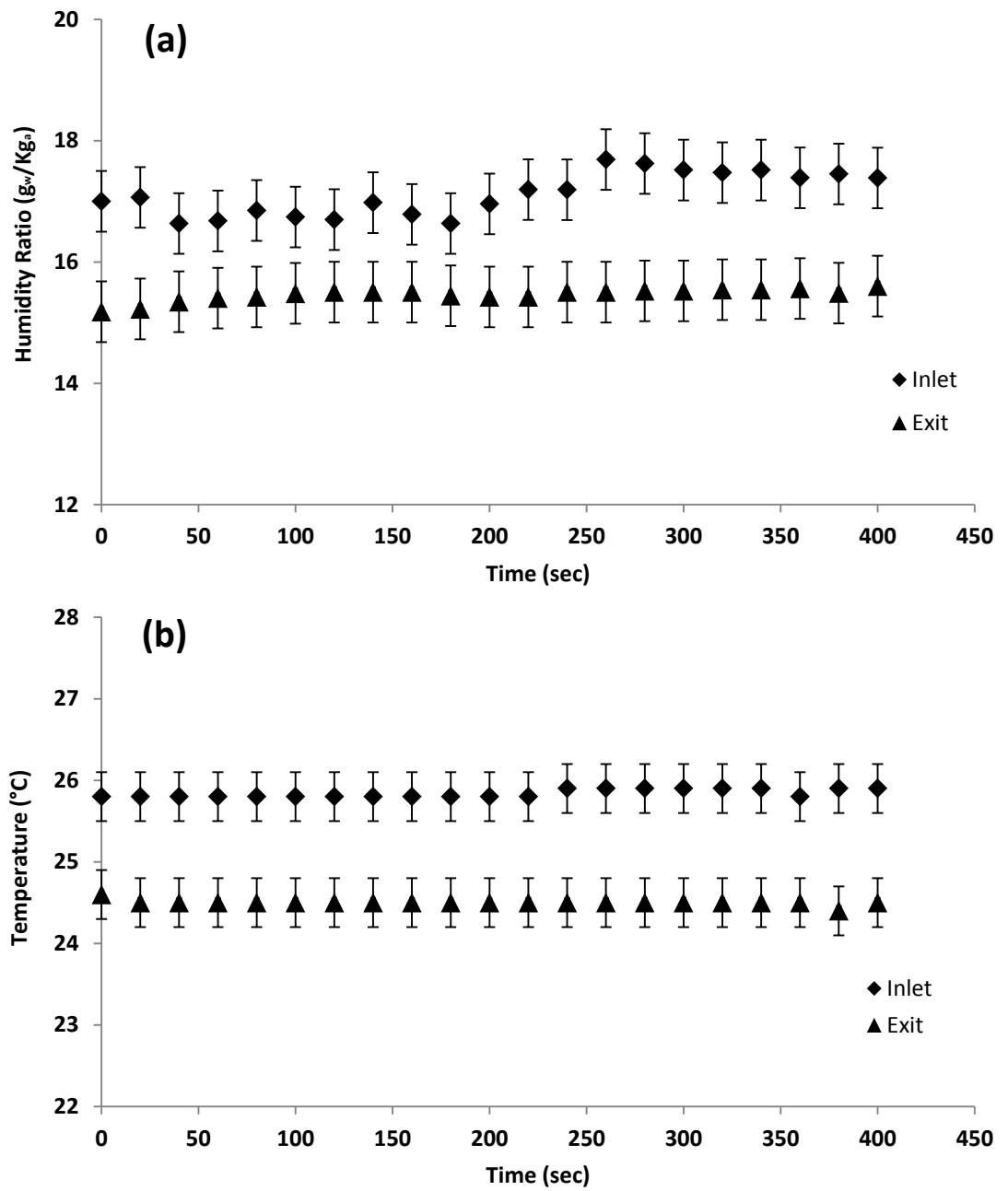


Figure 9: The inlet and exit conditions to the dehumidifier; (a) Humidity ratio and (b) Temperature

To validate the theoretical framework, the average inlet conditions to the regenerator and dehumidifier were used as inputs to the model. To run the mathematical model, the membrane material properties should be known, which were taken as  $5.2 \times 10^{-7} \text{ m}^2/\text{s}$  for the material vapor diffusivity and 0.34 W/mk for the thermal conductivity (Vashistha, et

al., 2013). The predictions of the analytical model and the actual experimental results are summarized in table 1.

Table 1: Comparison between experimental and theoretical

	Inlet Conditions		Exit Theoretical		Exit Experimental	
	Temperature (°C)	Humidity Ratio (g <sub>w</sub> /Kg <sub>a</sub> )	Temperature (°C)	Humidity Ratio (g <sub>w</sub> /Kg <sub>a</sub> )	Temperature (°C)	Humidity Ratio (g <sub>w</sub> /Kg <sub>a</sub> )
Dehumidifier	25.88 ± 0.3	17.45 ± 0.65	26.1	14.5	24.5 ± 0.3	15.33 ± 0.6
Regenerator	24.52 ± 0.3	12.38 ± 0.54	30.54	15.28	31.13 ± 0.33	14.70 ± 0.62

As shown in table 2, the model was able to predict the exit conditions. The error in predicting the temperature was 6.5% in the dehumidifier and 2% in the regenerator. As for the humidity ratio, the error was 5.4% in the dehumidifier and 4 % in the regenerator.

In order to check the moisture balance of the setup, i.e. the moisture desorbed by the regenerator is equal to that absorbed by the dehumidifier; a moisture balance was made on both devices. The moisture balance was performed using average values for the inlet and exit conditions of the regenerator and dehumidifier. The mass absorbed/desorbed is calculated using equation 15.

$$m_g = m_a (\omega_{in} - \omega_{out}) \quad (15)$$

The rate of moisture absorption by the dehumidifier is found to be  $2.37 \times 10^{-3}$  g/s while that of the regenerator was  $2.6 \times 10^{-3}$  g/s. The error in the value is 9.7 % of the value desorbed in the dehumidifier. This error is within the total experimental setup accuracy. The experimental results show that the model predicts well the performance of the regenerator and the dehumidifier. At the end of the experiment the concentration

in the tanks did not change and remained at the initial value of 38 %, as measured by the titration technique HACH 8225 for chloride and HACH 8226 for calcium hardness (2008)

## CHAPTER IV

### CASE STUDY

#### A. System Description

In order to test the efficiency of the membrane desiccant cycle, it will be applied to an internal office space, of dimensions  $3 \times 6 \times 7$  m, in the city of Beirut. As mentioned earlier, Beirut is a coastal city; hence sea water at  $17^\circ\text{C}$  can be used as a heat sink to supply the required cooling loads (Audah, et al., 2011).

The office under study has a typical latent and sensible load profile shown in table 2. The membrane desiccant system will be used as the primary system to lower the humidity level in the office. The dehumidification pipes of the system will be installed in a vertical manner on one of the room walls. To ensure efficient dehumidification, the length of the pipes will be equal to the room height, which is 3 m. The total number of pipes used is 190, covering the wall area, each with an outer diameter of 2.3 cm, similar to the one used in the experiment. The large number of dehumidification tubes considered is to ensure that there is sufficient mass transfer area between the liquid desiccant in the tubes and the room air.

The indoor space is conditioned by 100 % fresh air. Using the heat sink at  $17^\circ\text{C}$ , the fresh air temperature is lowered from the external ambient temperature to a temperature of  $18^\circ\text{C}$ . If the dew point temperature of the ambient air is higher than  $18^\circ\text{C}$  (which is typical for a summer day in Beirut City), the supply air will enter at 100% relative humidity and  $12.52 \text{ g}_w/\text{Kg}_a$  humidity ratio. The corresponding supply air flow rates needed to maintain a room temperature around  $24^\circ\text{C}$  are shown in table 2.

Table 2: Internal loads and Ambient Conditions

	Internal Sensible Load -Watts	Internal Latent Load -Watts	Supply Air Flow rate Kg/s	Ambient Temperature °C	Ambient Humidity Ratio $g_w/Kg_a$	Solar Flux -Watts
8:00-9:00	987	128	0.16	29	17.02	512
9:00-10:00	987	128	0.16	30	18.06	653
10:00-11:00	987	128	0.16	30	18.06	754
11:00-12:00	1554	256	0.22	31	19.15	798
12:00-1:00	1554	256	0.22	31	19.15	780
1:00-2:00	1554	256	0.22	30	18.06	701
2:00-3:00	1392	220	0.20	31	19.15	574
3:00-4:00	1392	220	0.20	31	19.15	419
4:00-5:00	1392	220	0.20	31	19.15	256

As for the liquid desiccant entering the room through the pipes, a dehumidification temperature of 23°C and concentration of 40% is chosen ensuring dehumidification (Abdel-Salam, et al., 2014). The desiccant mass flow rate is set at of 3.6 kg/hr per pipe (Rattner, et al., 2011) (Bergero, et al., 2001) . As for the regeneration tubes, their number and diameter is equal to that of the dehumidification pipes placed in the indoor area, i.e. 190 tube and 2.3 cm respectively. Their length however is reduced from 3 m to 1 m to prevent excessive drop in the desiccant temperature upon interacting with the ambient air, due to the low desiccant flow rate in the tubes.

The regeneration thermal energy required by the membrane system will be supplied through the use of parabolic solar panels and a storage tank. The parabolic solar panels will be sized according to the thermal energy consumption required by the desiccant to raise its temperature to the regeneration temperature, with the provision that the solar panels area does not cover more than 40% of the roof area.

## 1. Results and Performance

The model will be simulated for a typical day in August, with the ambient conditions shown in table 2. To evaluate the performance of the system and its efficiency in removing humidity from indoor space, the room model will be simulated with and without the membrane desiccant system. The hourly variation of the room temperature, humidity ratio and relative humidity with and without the system are shown in figures 10, 11 and 12 respectively, whereas the hourly thermal energy needed for the regeneration of the desiccant is shown in Fig. 13.

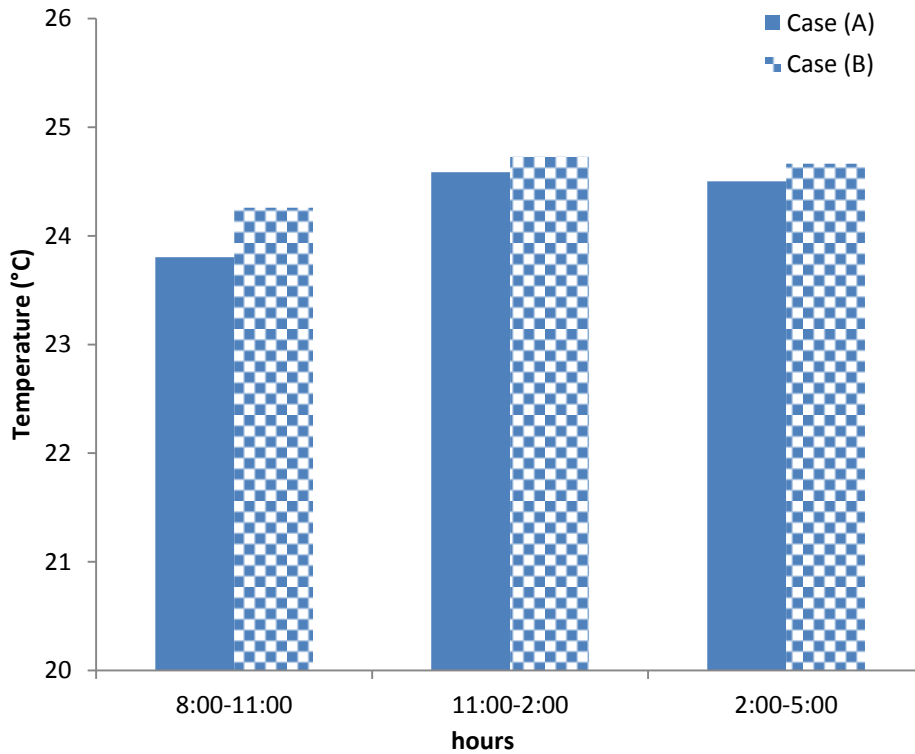


Figure 10: Indoor temperature variation; case (A) without the membrane system, case (B) with the membrane system

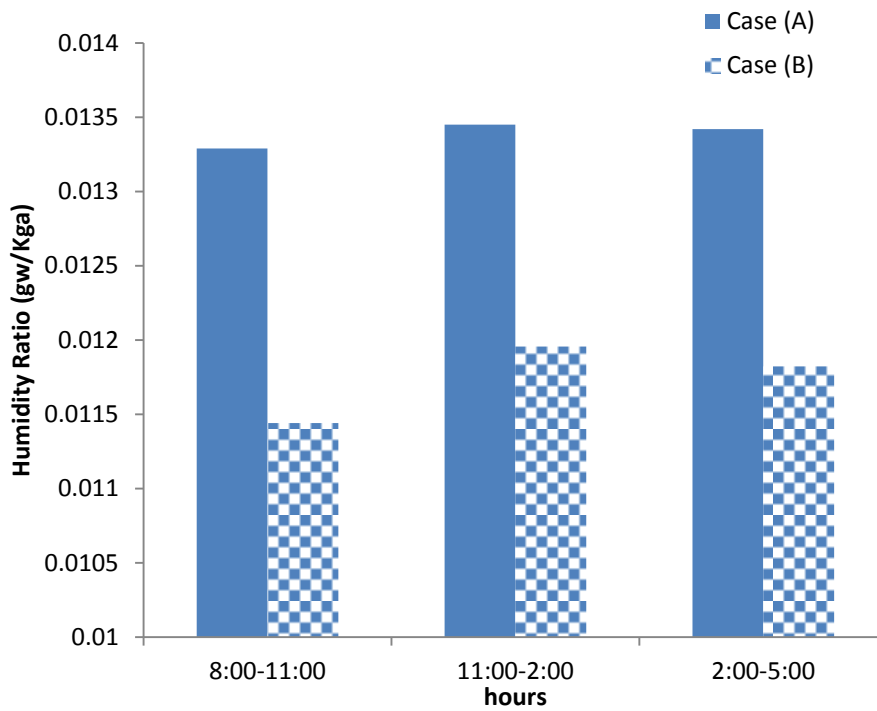


Figure 11: Indoor humidity ratio variation; case (A) without the membrane system, case (B) with the membrane system

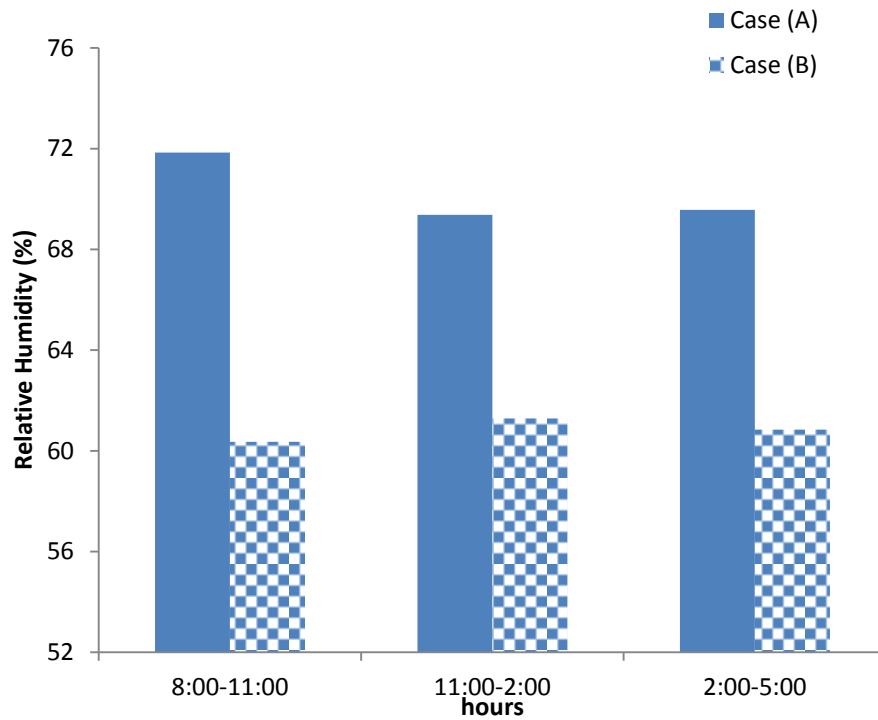


Figure 12: Indoor relative humidity variation; case (A) without the membrane system, case (B) with the membrane system

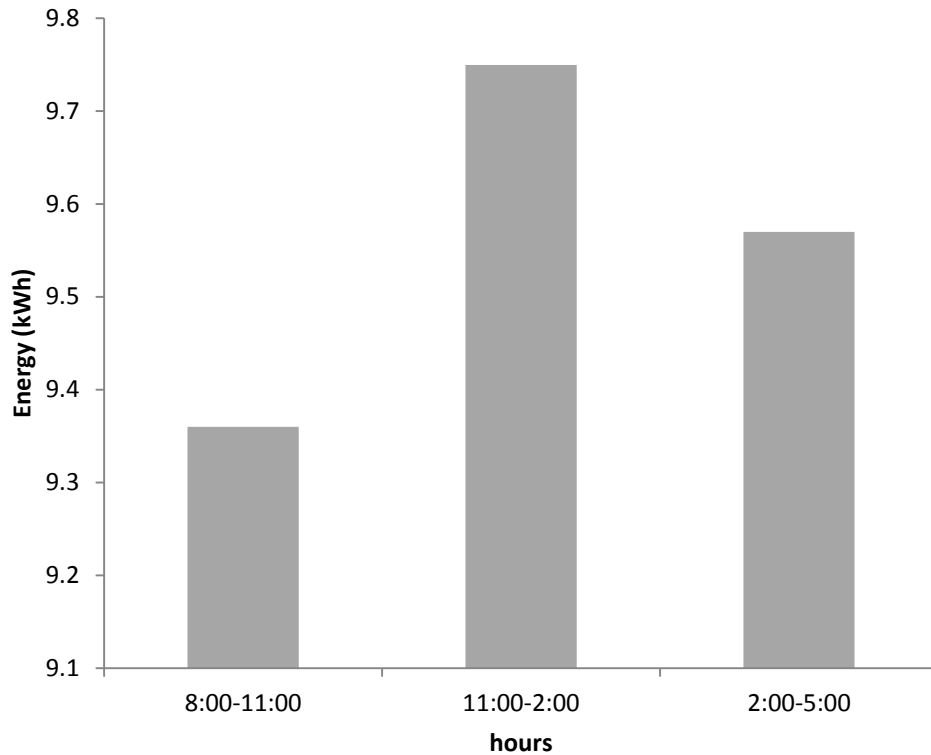


Figure 13: Thermal energy consumption of the membrane desiccant system with respect to time

## 2. Discussion

In case (A), i.e. in the absence of the membrane system, the conditioned air was able to maintain a good comfort temperature but not a good relative humidity. The indoor air temperature for case (A) was on average 24.2°C ranging between 23.8°C and 24.5°C and reaching a peak value at noon time in accordance with the sensible load, as shown in Fig. 10. The average value of the humidity ratio was 13.38 g<sub>w</sub>/Kg<sub>a</sub>, which was higher than the supply air humidity ratio of 12.52 g<sub>w</sub>/Kg<sub>a</sub> due to the latent load in the room. The humidity ratio reached a peak of 13.45 g<sub>w</sub>/Kg<sub>a</sub> during the noon, when the latent load was the highest as shown in Fig. 11. The relative humidity achieved in case (A) was on average 70.2 %, where its highest value was 71.8 % during the morning, due to



the low temperature of the indoor space and then it decreased throughout the day due to the increase in the temperature of indoor air, as shown in Fig. 12.

For case (B), i.e. in the presence of the desiccant system, the room temperature slightly increased throughout the day by an average value of  $0.25^{\circ}\text{C}$ , as shown in Fig. 10. The slight increase in the room temperature is due to vapor absorption along the length of the pipes. The absorption energy associated with moisture removal increased the liquid desiccant temperature in the tubes which in turn heated slightly the indoor air. However this effect has minimal impact on the indoor space temperature where the increase is only 1% of the room temperature. As for the humidity ratio of the indoor air, in case (B) it was consistently lower than that of case (A), as shown in Fig. 11. The difference between the average humidity ratio of the liquid desiccant,  $\omega_{sol}^*$  of  $7.7 \text{ g}_w/\text{Kg}_a$ , and the room air is the driving potential for moisture absorption through the permeable membrane. The average humidity ratio of the indoor air was  $11.7 \text{ g}_w/\text{Kg}_a$  where it ranged from  $11.44 \text{ g}_w/\text{Kg}_a$  to a peak value of  $11.95 \text{ g}_w/\text{Kg}_a$  during midday. The jump in the value of the room humidity ratio is attributed to two factors. The first is the increase of the latent load during midday and the second is the increase of the flow rate of the humid supply air during midday, which was necessary to maintain an indoor temperature around  $24^{\circ}\text{C}$ . The indoor air relative humidity in case (B) was on average 60% as compared to a value of 70% for case (A), as shown in Fig. 12. Due to the slight increase in the room temperature and due to the substantial reduction in the room humidity ratio, the membrane system has helped in stabilizing the relative humidity value around 60% throughout the day. The indoor humidity ratio, relative humidity and temperature achieved in case (B), i.e. in the presence of the membrane system, are within the acceptable thermal comfort zone as set by ASHRAE Standard 55, which

recommends a strict upper limit of 0.012 Kg<sub>w</sub>/Kg<sub>a</sub> for humidity ratio, a relative humidity between 56 % and 67% and a temperature between 24 and 28°C during the summer (Turner, 2011).

The thermal energy consumption of the membrane desiccant system is shown in Fig.13. The energy consumption of the system was low during the beginning of the day, it peaked during mid-day and then it decreased towards the end. This is in accordance with the ambient humidity ratio variation. As the humidity of the ambient increases, the regeneration temperature of the desiccant will increase in order to raise the desiccant humidity ratio,  $\omega_{sol}^*$ . Due to the low flow rate of the desiccant used, the system generally consumes relatively low thermal energy (around 3.2 kW per hour as a mean value).

## **B. Economic Analysis**

### ***1. Energy Consumption of Vapor Compression System vs. Membrane System***

To estimate the economic feasibility and efficiency of the membrane desiccant system, it will be compared to a conventional vapor compression system that can attain the same indoor conditions (temperature and relative humidity) as that of the membrane system. The comparison is done over a period of five month consisting of May, June, July, August and September, which represent the most humid months of Beirut City and which require efficient dehumidification.

The vapor compression cycle used has a COP of 3. It will first subcool the supply air to reach the required humidity ratio, and then through the use of an electric heating coil, the supply air will be reheated to the adequate supply temperature. For the

office space considered in August and simulated in section 7.2, the subcool electric energy and the reheat energy required during one day, are shown in table 3. A total daily electric energy consumption of 8 kWh is consumed by the vapor compression cycle in the reheat-subcool process. This amount will not change throughout the considered period of five month since the loads are mostly internal and the supply conditions to the room are the same.

Table 3: Energy loads for the Membrane Desiccant System and Conventional System

	Subcool energy (kWh)	Electric energy required for the subcool (kWh)	Reheat electric energy (kWh)	Total electric energy (kWh)
8:00-11:00	3.67	1.223	1.39	2.613
11:00-2:00	4.061	1.354	1.37	2.724
2:00-5:00	3.96	1.32	1.343	2.663
Total Energy per day	11.691	3.897	4.103	8.00

The average ambient temperatures during the considered months is above 24°C and the dew temperature of the air is on average higher than 18°C, thus the supply conditions to the room will not change and hence the amount of 8 kWh will not vary. Over a period of five month the total electric energy consumption will be 1372.5 kWh.

As for the membrane system, the ambient conditions are varying every month, and hence the regeneration temperature of the desiccant will vary accordingly, since the membrane desiccant system is desorbing the moisture to the ambient environment. To estimate the regeneration energy of the desiccant, a representative day was taken for each month and the model was simulated. The thermal energy requirement for each month is shown in Fig. 14.

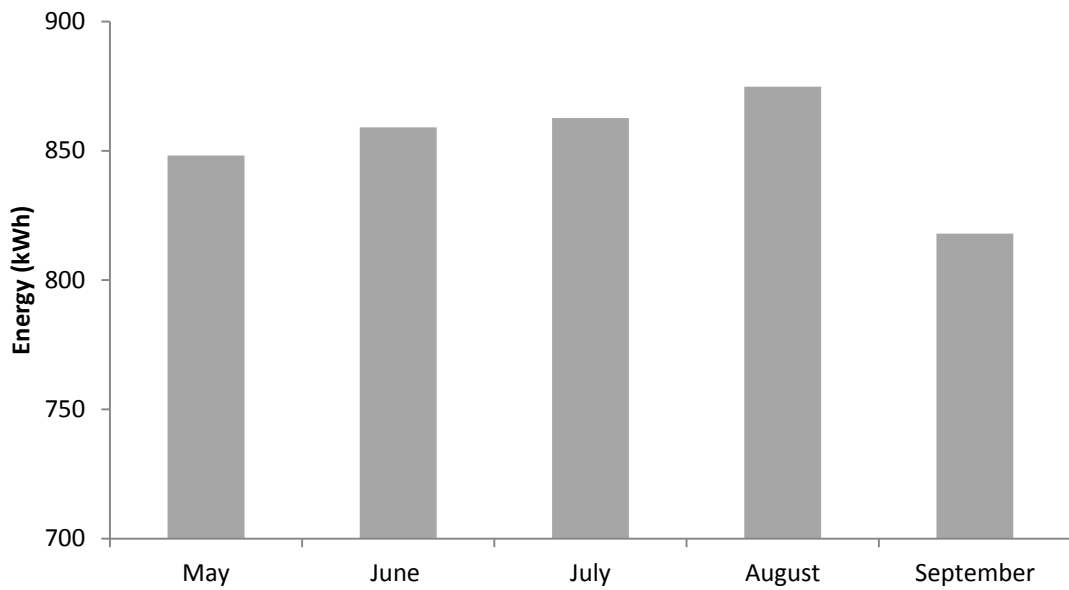


Figure 14: Monthly thermal consumption of the membrane desiccant cycle

The thermal energy consumption increases in accordance with the months of highest humidity ratio. As the ambient humidity ratio increases, the regeneration temperature of the desiccant increases and hence the thermal energy requirement of the cycle increases. Having established the thermal load of the membrane desiccant system, the parabolic solar panels and the storage tank can be sized accordingly. A total of  $4.8 \times 1.2$  m parabolic collectors along with a  $1 \text{ m}^3$  storage tank can supply the required thermal energy of the system, given the solar flux profile shown in table 2. The total surface area of the solar panels and the storage tank cover an area that does not exceed 20 % of the roof surface area. Table 4 shows the specification of a single parabolic module (Audah, et al., 2011). Using the design parameters of the parabolic system, membrane cycle thermal loads and ambient conditions, the storage tank and parabolic collectors model is simulated. The temperature variation of the storage tank and the solar flux are shown in Fig. 15. During the first hour of operation, 8:00, the temperature of the tank decreases slightly due to the high thermal load and low solar flux as shown in Fig. 15. During

midday, the solar flux increases and the temperature of the tank follow with a time lag due to the capacitance of the tank.

Table 4: Solar system specifications

Design Parameter	Value
<i>Tank specifications</i>	
Tank volume	1 m <sup>3</sup>
Tank total surface area	5.545 m <sup>2</sup>
Loss coefficient of tank	0.5 W/m <sup>2</sup> k
<i>Parabolic Solar Module specifications</i>	
Collector tube diameter	0.06 m
Transparent cover tube diameter	0.09 m
Flow rate of water in collector	0.0535 Kg/s
Width of the collectors	1.2 m
Length of the collectors	2.4 m

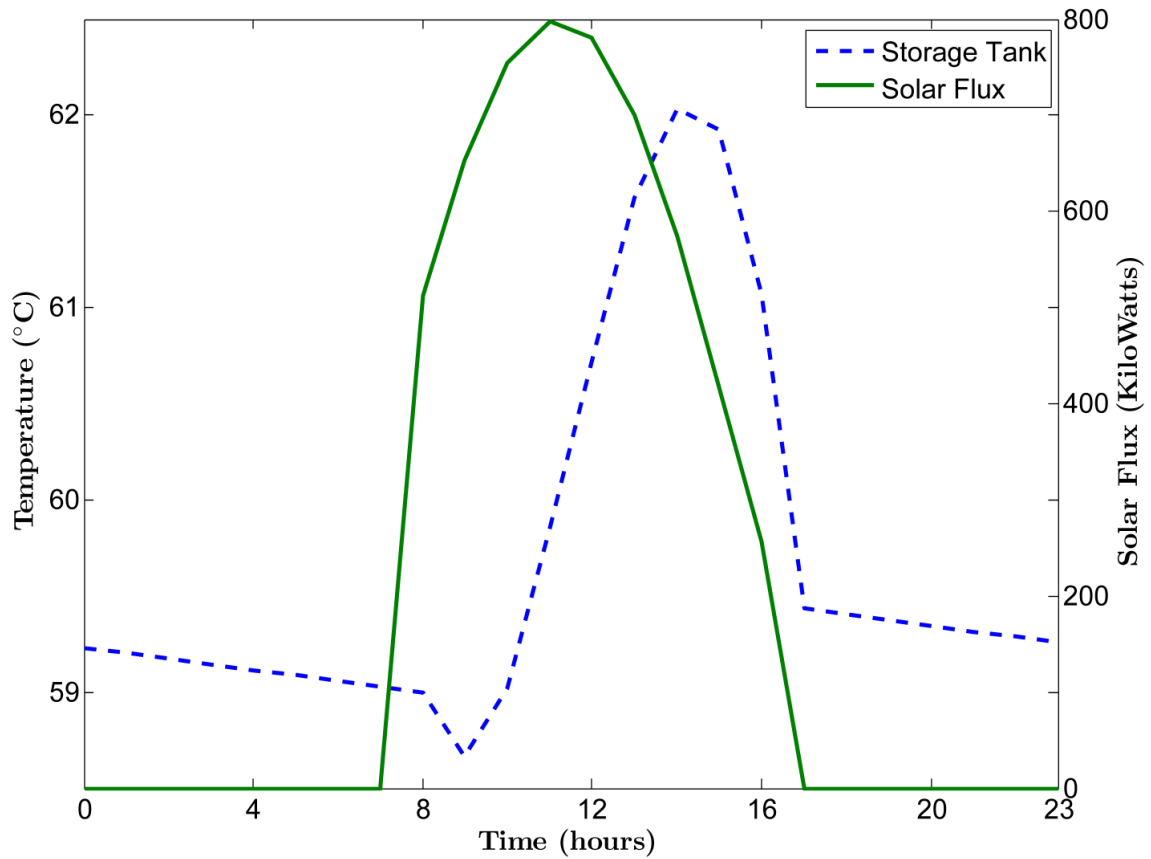


Figure 15: Storage tank temperature and solar flux hourly variation

## ***2. Economic analysis of energy consumption***

The goal of the current economic analysis is to determine the payback period, using present worth analysis, which the consumer has to wait in order to return the money invested in the cost of the membrane system and the parabolic solar collectors. The cost of installing the membrane system will be compared to the cost of installing the vapor compression cycle in addition to the cost of electric energy consumed every year.

The cost of the membrane system includes the initial costs of the dehumidification/regeneration pipes and the parabolic solar panels. The total length of parabolic collectors required to supply the monthly regeneration energy of the membrane desiccant is 4.8 m with a width of 1.2 m. The estimated cost of the parabolic collectors is \$ 2000 (Audah, et al., 2011). As for the membrane itself, the material used, which is Propore<sup>®</sup>, costs \$ 5/m<sup>2</sup> (Larson, 2006), which implies a total material cost of \$ 400. The cost of installation and fabrication of the membrane pipes is estimated as \$ 500. Therefore the total cost of the membrane-desiccant system is \$ 2900.

Considering a commercially available vapor compression system, the initial installation cost is estimated as \$ 800, whereas the cost of electricity in Beirut City is estimated as 0.19 \$/kWh. Therefore the cost of electricity consumption by the vapor compression cycle over the operational period of 5 month per year is calculated to be \$ 261.

In order to determine the present worth value of both systems formulas (8) and (9) are used.

$$P = A_0 \frac{1 - \left(\frac{1+i}{1+d}\right)^n}{d-i} \quad i \neq d \quad (8)$$

$$P = A_0 \frac{n}{1+d} \quad i=d \quad (9)$$

In equations (7) and (8), P represents the present worth, n the number of years, d the discount rate and i the annual rate at which electricity costs are increasing. Using a discount rate of 2% and an annual rate of electricity price increase as 3 %, the payback back period after which the initial investment in the solar collectors and the membrane system is returned to the costumer is 7 years and 8 month.

This is a relatively long payback period. It can be justified that the system is operating for a period of 5 month per year. Other membrane systems that have been studied in literature have a payback period of 4-6 years (Abdel-Salam, et al., 2014).

### C. Conclusion and Future Work

In this study, the performance and feasibility of a membrane desiccant system integrated with solar energy has been evaluated. A theoretical model has been proposed to integrate the indoor room model with the membrane desiccant system and the parabolic solar collectors. Experiments were performed to validate the theoretical model. The predictions of the theoretical model were in good agreement with the experimental findings. After the validation, the system was applied to a test case for a typical internal office space in Beirut City. The results showed that the system can

achieve indoor thermal comfort with minimal effects on room temperature. A drop of 10% of indoor relative humidity was observed when the system was installed. The economic cost of the membrane desiccant system was then compared to a conventional vapor compression cycle that can achieve the same indoor conditions as the desiccant system, in the presence of a heat sink. The cost of the vapor compression cycle in addition to the electricity consumption each year was compared to the initial cost of the solar panels and the membrane system. The payback period to return the initial cost of the investment was estimated, using present worth analysis, and was found to be 7 years and 8 month. The long payback period is due to the fact that for an office in Beirut city, the system operates only for 5 month per year, as compared to other locations in the globe which need throughout the year dehumidification.

#### *Significance of the Project*

This study proposes a fully operated system on sustainable energy. It uses the solar radiation as the source of regeneration energy for the liquid desiccant and the available heat sink as a cooling source, which makes it a fully passive system. The main addition over traditional liquid desiccant cycles (Mohammad, et al., 2013) is that dehumidification is done directly in the indoor room without the need of dehumidification towers with beds or regenerators. This is more compact than traditional liquid desiccant cycles- and even solid desiccant cycles, which use relatively large desiccant wheels- and can be installed in residential buildings. It is similar to the HAMP system (Fauchoux, et al., 2010), but the addition is the coupling with the full cycle to regenerate the desiccant which has not been done before.

High moisture levels, as stated earlier, can impose serious implication on our daily life, especially in humid zones such as Beirut and the coastal areas of the



Mediterranean. This fact added to the increase in energy production and consumption and global warming and other environmental, economical, and sustainability issues, requires operational devices that use minimal energy. This system provides a viable and a low cost- on the short and long run- alternative.

## BIBLIOGRAPHY

*HACH Water Analysis Handbook Procedures* (5th ed.). (2008).

Abdel-Salam, A. H., & Simonson, C. J. (2014). Annual evaluation of energy, environmental and economic performances of a membrane liquid desiccant air conditioning system with/without ERV. *Applied Energy*, *116*, 134-148.

Audah, N., Ghaddar, N., & Ghali, K. (2011). Optimized solar-powered liquid desiccant system to supply building fresh. *Applied Energy*, *88*, 3726-3736.

Bergero, S., & Chiari, A. (2001). Experimental and theoretical analysis of air, humidification/dehumidification process using hydrophobic capillary contractors. *Applied Thermal Engineering*, *21*, 1119-1135.

Bradshaw, V. (2006). *The Building Environment: Active and Passive Controls* (Third ed.). John Wiley & Sons, Inc.

Chenvidyakarn, T. (2007). Review Article: Passive Design for Thermal Comfort in Hot Humid Climates. *Journal of Architectural/Planning Research and Studies*, *5*.

Conde, M. R. (2004). Properties of aqueous solutions of lithium and calcium chloride: formulations for use in air conditioning equipment design. *International Journal of Thermal Sciences*, *43*, 367-382.

Dougherty, E. (2011). *WHY DO WE SWEAT MORE IN HIGH HUMIDITY?* Retrieved from <http://engineering.mit.edu/ask/why-do-we-sweat-more-high-humidity>

Duffie, J. A., & Beckman, W. A. (n.d.). *Solar Engineering and of Thermal Processes*. JOHN WILEY & SONS, INC.

- Eldeeb, R., Fauchoux, M., & Simonson, C. J. (2013). Applicability of a heat and moisture transfer panel (HAMP) for maintaining space relative humidity in an office building using TRNSYS. *Energy and Buildings*, 66, 338-345.
- Elsayed, M., Gari, H. N., & Radhwan, A. (1993). Effectiveness of heat and Mass transfer in packed beds of liquid desiccant system. *Renewable Energy*, 3, 661-668.
- Fan, H., Carey j. Simonson, R. W., & Shang, W. (2006). Performance of a Run-Around system for HVAC Heat and Moisture Transfer Applications Using Cross-Flow Plate Exchangers Coupled with Aqueous Lithium Bromide. *HVAC & R Research*, 12(2), 313-336.
- Fauchoux, M., Bansal, M., PrabalTalukdar, Simonson, C. J., & Torvi, D. (2010). Testing and modelling of a novel ceiling panel for maintaining space relative humidity by moisture transfer. *International Journal of Heat and Mass Transfer*, Volume 53, Issues 19–20, 53, 3961-3968.
- Fauchoux, M., Simonson, C., & Torvi, D. (2009). Tests of a Novel Ceiling Panel for Maintaining Space Relative Humidity by Moisture Transfer from an Aqueous Salt Solution. *ASTM International*, 6.
- Fumo, N., & Goswami, D. (2002). Study of an aqueous lithium chloride desiccant system: air dehumidification and desiccant regeneration. *Solar Energy*, 72, 351-361.
- Ghaddar, N., Ghali, K., & Najm, A. (2004). Use of desiccant dehumidification to improve energy utilization in air-conditioning systems in Beirut.

- Ghali, K., Katanani, O., & Al-Hindi, M. (2011). Modeling of the effect of hygroscopic curtains on relative humidity for spaces air conditioned by DX split air conditioning system. *Energy and Buildings*, *43*, 2093-2100.
- Hemingson, H. B., Simonson, C. J., & Besant, R. W. (2011). Steady-state performance of a run-around membrane energy exchanger(RAMEE) for a range of outdoor air conditions. *International Journal of Heat and Mass Transfer*, *54*, 1814-1824.
- Incropera, D., & Bergman, L. (n.d.). *Fundamentals of Heat and Mass Transfer*.
- La, D., Dai, Y., Li, Y., Wang, R., & Ge, T. (2010). Technical development of rotary desiccant dehumidification and air conditioning: A review. *Renewable and Sustainable Energy Reviews*, *14*, 130-147.
- Larson, M. D. (2006). *The performance of membranes in a newly proposed runaround heat and moisture exchanger*.
- Mahmud, K., Mahmood, G. I., Simonson, C. J., & Besant, R. W. (2010). Performance testing of a counter-cross-flow run-around membrane energy exchanger (RAMEE) system for HVAC applications. *Energy and Building*, *42*, 1139-1147.
- Moghaddam, D. G., LePoudre, P., Besant, R. W., & Simonson, C. J. (2013). Steady-State Performance of a Small-Scale Liquid-to-Air Membrane Energy Exchanger for Different Heat and Mass transfer Directions, and Liquid Dessicant Types and Concentrations: Experimental and Numerical Data. *Journal of Heat Transfer*, *135*.
- Mohammad, A. T., Mat, S. B., Sulaiman, M., Sopian, K., & A.Al-abidi, A. (2013). Historical review of liquid desiccant evaporation cooling technology. *Energy and Buildings*, *67*, 22-33.

- Morse, R. G., Haas, P. E., & Zehnter, D. A. (2007). Causes and Effects of High Humidity in South Florida Schools. *ASHRAE Building X International Conference*.
- Pa'tek\*, J., & Klomfar, J. (2006). A computationally effective formulation of the thermodynamic properties of LiBr-H<sub>2</sub>O solutions from 273 to 500 K over full composition range.
- Radhwan, A., Gari, H., & Elsayed, M. (1993). Parametric Study of a Packed Bed Dehumidification/Regenerator Using CaCl<sub>2</sub> Liquid Desiccant. *Renewable Energy*, 49-60.
- Rattner, A. S., Nagavarapu, A. K., Garimella, S., & Fuller, T. F. (2011). Modeling of a flat plate membrane-distillation system for liquid desiccant regeneration in air-conditioning applications. *International Journal of Heat and Mass Transfer*, 54, 3650-3660.
- Straube, J. (2002). Moisture in Buildings. *ASHRAE Journal*.
- Studak, J. W., & Peterson, J. L. (1988). A Preliminary Evaluation of Alternative Liquid Desiccants for a Hybrid Desiccant Air Conditioner. *Proceedings of the Fifth Symposium on Improving Building Systems in Hot and Humid Climates*.
- Turner, S. C. (2011). What's New in ASHRAE's Standard on Comfort. *ASHRAE Journal*.
- Vashistha, V., & Talukdar, P. (2013). Numerical studies for performance evaluation evaluation of a permeable ceiling panel for regulation of indoor humidity. *Energy and Buildings*, 62, 158-165.

Wilson, A. (2003). *Moisture Control in Buildings: Putting Building Science in Green Building*. Retrieved from

<http://www.buildinggreen.com/auth/article.cfm/2003/7/1/Moisture-Control-in-Buildings-Putting-Building-Science-in-Green-Building/>

Yassine, B., Ghali, K., Ghaddar, N., Srour, I., & Chehab, G. (2012). A numerical modeling approach to evaluate energy-efficient mechanical. *Energy and Buildings*, 55, 618-630.

## Appendix I

### TIME PLAN

Project plan for the year of 2013	June	July	August	September	October	November	December
1. Literature review of moisture and heat transport in porous media in context of hygroscopic curtains and numerical simulations							
2. Literature review of liquid desiccant dehumidification technology, thermosyphone modal, and permeable membranes							
3. Development of the theoretical model for heat and moisture transport in cylindrical micro porous polypropylene pipes							
4. Simulations for the different dehumidification setups and different system arrangements							

Project plan for the year of 2014	January	February	March	April	May	June	July
5. Set the goals for the final system setup and develop the theoretical modal for the dehumidification cycle							
6. Run simulations for system modal at steady state							
7. Perform the experiment on the regenerator and dehumidifier							
8. Compare the experimental results with the theoretical modal and update the theoretical modal							
9. Present the results							

## Appendix II

### CaCl<sub>2</sub>-H<sub>2</sub>O SOLUTION THERMODYNAMIC PROPERTIES

#### A. Specific heat of the liquid desiccant, CaCl<sub>2</sub> – H<sub>2</sub>O

A corollation for the variation of specific heat of the CaCl<sub>2</sub> – H<sub>2</sub>O solution for various temperatures and concentrations is found in (Conde, 2004) The formula uses the specific heat of pure water with correction factors due to the existence of the salt, CaCl<sub>2</sub>. The specific heat of pure water is shown in the following equation.

$$c_{p,H_2O}(\theta) = A + B\theta^{0.02} + C\theta^{0.04} + D\theta^{0.06} + E\theta^{1.8} + F\theta^8 \quad (2)$$

Where  $\theta = \frac{T}{228} - 1$ , and T is in kelvin. The coefficients used in equation (2) are shown in the following table.

	A	B	C	D	E	F
$\theta \leq 0^\circ C$	830.546	-1247.52	-68.6	491.2765	-1.8069	-137.515
$\theta > 0^\circ C$	88.7891	-120.1958	-16.9264	52.4654	0.10826	0.46988

The specific heat of the liquid desiccant is shown in the following equation.

$$c_{p,sol}(T, \xi) = c_{p,H_2O}(T) \times (1 - f_1(\xi) \times f_2(T)) \quad (1)$$

Where  $f_1(\xi) = A\xi + B\xi^2 + C\xi^3$

$f_2(T) = F\theta^{0.02} + G\theta^{0.04} + H\theta^{0.06}$

And the coefficients are given in the following table:

A	B	C	F	G	H
1.63799	-1.69002	1.05124	58.5225	-105.6343	47.7948

$\xi$  is the mass concentration of the liquid desiccant solution.



## B. Enthalpy of dilution of the liquid desiccant, $\text{CaCl}_2 - \text{H}_2\text{O}$

The enthalpy of dilution is the energy generated by the absorption of the water vapor molecules by the desiccant solution. The absorption process is an exothermic process. The enthalpy of dilution is also the heat released upon mixing of the calcium chloride salt initially with water. It is given by the following formulas.

$$\zeta = \frac{\xi}{H_4 - \xi}$$

$$\Delta h_{d,0} = H_5 + H_6 \theta$$

$$\Delta h_d = \Delta h_{d,0} \left[ 1 + \left( \frac{\zeta}{H_1} \right)^{H_2} \right]^{H_3}$$

$H_1$	$H_2$	$H_3$	$H_4$	$H_5$	$H_6$
0.855	-1.965	-2.265	0.8	-955.69	3011.974

### C. Enthalpy of the liquid desiccant, $CaCl_2 - H_2O$

The enthalpy of the liquid desiccant is not found in a complete correlation as the specific heat and the enthalpy of dilution. The following formula is used to calculate the enthalpy, at the desiccant temperature  $T$  and the concentration per dry basis,  $c$ , taking pure liquid water at 273.15 k as a reference state:

$$h_{sol}(T, c) = \int_{273.15}^T c_{p,sol}(T, c) dT - \Delta h_d(273.15, c)$$

Where  $c$  is the concentration. Since solving for the cycle requires iterations, and performing the integral at every time the enthalpy needs to be evaluated consumes time, the previous equation has been calculated for a range of temperatures and concentrations and the following correlation has been used in the simulations with a maximum of 5% error from the previous equation:

$$h_{sol}(T, z) = p_{00} + p_{10}z + p_{01}T + p_{20}z^2 + p_{11}zT + p_{02}T^2 + p_{30}z^3 + p_{21}z^2T + p_{12}zT^2 + p_{03}T^3 + p_{40}z^4 + p_{31}z^3T + p_{22}z^2T^2 + p_{13}zT^3$$

$Z$  is the mass concentration of the desiccant solution;  $z=1/(1+c)$ .

p00	-1.329e+06
p10	4.713e+06
p01	4223
p20	-6.925e+06
p11	-1.564e+04
p02	-0.6276
p30	2.889e+06
p21	7031
p12	25.34
p03	0.001053
p40	1.827e+06
p31	-3823
p22	-1.401

#### D. Humidity ratio of the liquid desiccant, $CaCl_2 - H_2O$

The surface humidity ratio of the liquid desiccant is calculated according to the following formula:

$$\omega_{sol}^*(T, c) = 0.622 \frac{P_v}{P_{tot} - P_v}$$

where  $p_v$  is the partial pressure of water vapor at the surface of the liquid desiccant at the desiccant's temperature and concentration and is calculated according to the following correlation:

$$p_v(T, \xi) = \pi_{25} f(\xi, \theta) p_{H_2O}(T)$$

$$f(\xi, \theta) = A + B\theta$$

$$A = 2 - \left[ 1 + \left( \frac{\xi}{\pi_0} \right)^{\pi_1} \right]^{\pi_2}$$

$$B = \left[ 1 + \left( \frac{\xi}{\pi_3} \right)^{\pi_4} \right]^{\pi_5} - 1$$

$$\pi_{25} = 1 - \left[ 1 + \left( \frac{\xi}{\pi_6} \right)^{\pi_7} \right]^{\pi_8} - \pi_9 e^{-\frac{(\xi-0.1)^2}{0.005}}$$

$\pi_0$	0.31
$\pi_1$	3.698
$\pi_2$	0.60
$\pi_3$	0.231
$\pi_4$	4.584
$\pi_5$	0.49
$\pi_6$	0.478
$\pi_7$	-5.20
$\pi_8$	-0.40
$\pi_9$	0.018

$p_{H_2O}(T)$  is the saturation pressure of water at temperature T and is calculated according to the following correlation:

$$p_{sat}(T) = p_c \exp\left(\frac{T_c}{T} \sum_i a_i \left(1 - \frac{T}{T_c}\right)^{b_i}\right)$$

$T_c = 647.096$  and  $p_c = 22.064e6$ ; the coefficients are shown in the following table:

$a_1$	-7.859517
$a_2$	1.844082
$a_3$	-11.7866497
$a_4$	22.6807411
$a_5$	-15.9618719
$a_6$	1.801225

$b_1$	1
$b_2$	1.5
$b_3$	3
$b_4$	3.5
$b_5$	4
$b_6$	7.5

## Appendix III

### CONVECTION COEFFICIENTS

#### **A. External heat convection coefficient of the permeable pipes placed in the indoor space**

The external heat convection coefficient of the pipes is calculated according to a cross flow of air perpendicular to the axis of the pipe with an average room velocity of sds the correlation used is the following:

for

$$0.1 < \text{Re} < 1000$$

$$Nu = 0.32 + 0.43(\text{Re})^{0.52}$$

$$1000 < \text{Re} < 50000$$

$$Nu = 0.24(\text{Re})^{0.6}$$

And  $\text{Re} = \frac{\rho_a v_a D_{outer}}{\mu_a}$ , where  $\rho_a$ ,  $v_a$ , and  $\mu_a$  are the density, velocity and viscosity of the air inside the room and  $D_{outer}$  is the outer diameter of the permeable tube.

$Nu = \frac{h_c D_{outer}}{k_a}$ , where  $k_a$  is the conductivity of air.

## **B. External heat convection coefficient of the permeable pipes used in the experimental setup**

Since the Reynolds number in the experimental setup is extremely low, the convection coefficient was calculated according to the following formula, which is used to calculate the convection coefficient between the HAMP (Fauchoux, et al., 2010) and the room air:

$$h_c = 2.13|T_p - T_a|^{0.31}$$

where  $T_p$  is the temperature of the permeable pipe and  $T_a$  is the temperature of the air flowing around it.

## **C. Internal heat convection coefficient of the permeable pipes**

The internal heat convection coefficient is calculated assuming a constant surface temperature and laminar flow in the pipes according to the following formula:

$$Nu = 3.66$$
$$h_c = \frac{3.66 \times k_w}{D_i}$$

where  $D_i$  is the internal pipe diameter and  $k_w$  is the conductivity of the liquid desiccant.

#### D. Mass convection coefficient

In order to calculate the internal and external mass convection coefficients the thermal diffusivity of air should be known, which is calculated according to the following formula:

$$\alpha = \frac{k_a}{\rho_a c_{p,a}}$$

Then the Lewis number is calculated.

$$Le = \frac{\alpha}{D_a}, \text{ where } D_a \text{ is the diffusion coefficient of water vapor in air.}$$

Then using the Colborn j factor and the analogy between heat and mass transfer, the mass convection coefficient is calculated according to the following formula:

$$h_m = h_c \frac{Le^{\frac{2}{3}}}{\rho_a c_{p,a}}, \text{ where } h_c \text{ is the heat convection coefficient, whether internal or}$$

external.

## Appendix IV

### CONSTANT RESISTANCE MODEL

The constant resistance model given by equation (3) is derived from the steady state energy equation applied in cylindrical coordinates, with heat flowing only in the radial direction; the details of the derivation can be found in (Incropera, et al.).

$$\frac{1}{r} \frac{d}{dr} \left( kr \frac{dT}{dr} \right) = 0$$

As for the constant mass resistance modal given by equation (4), it is derived from Fick's law applied also in cylindrical coordinates with mass flowing in the radial direction only as stated in the assumptions from which the model was derived. The details are shown also in (Incropera, et al.).

$$\frac{1}{r} \frac{d}{dr} \left( D \rho_a r \frac{d\omega}{dr} \right) = 0$$



Appendix V  
EXPERIMENT PICTURES



Figure 16: Photo showing the sensors placed across the dehumidifier



Figure 17: Heating tanks





Figure 18: Permeable pipes assembly in the regenerator/dehumidifier





Figure 19: Permeable pipes assembled in the dehumidifier

